THESIS FOR THE DEGREE OF DOCTOR OF PHILOSOPHY

Chemodynamical Simulations of Star-Forming Molecular Clouds

Chia-Jung Hsu

Department of Space, Earth, and Environment
Chalmers University of Technology
Gothenburg, Sweden, 2023

Chemodynamical Simulations of Star-Forming Molecular Clouds

Chia-Jung Hsu

ISBN: 978-91-7905-829-6
Doktorsavhandlingar vid Chalmers tekniska högskola
Ny series nr 5295
ISSN 0346-718X
This thesis has been prepared using LaTeX.

Department of Space, Earth, and Environment
Chalmers University of Technology
SE-412 96 Gothenburg, Sweden
Phone: +46 (0)31 772 1000
www.chalmers.se

Printed by Chalmers Reproservice
Gothenburg, Sweden, April 2023

Abstract

Stars are known to form from dense, dusty clumps and cores of molecular clouds. However, there is no consensus on a theory that can predict the rate of star formation, its clustering, and the conditions needed for massive stars to be born. A major challenge is how to observe and characterise the gas that is the fuel for star formation. One way is to take advantage of line emission from molecular species, a great variety of which have now been detected in the interstellar medium. However, interpreting the messages from these molecules necessitates an understanding and modeling of astrochemistry. In addition to this diagnostic power, astrochemistry is also expected to impact the physical evolution of the gas by influencing heating and cooling rates and controlling the degree of ionization, which mediates coupling to magnetic fields. To make progress in modeling the physical and chemical evolution of molecular clouds, we develop methods for chemodynamical simulations and carry out several studies combining magnetohydrodynamics (MHD) and astrochemistry. Our first investigation concerns the evolution of chemical abundances in massive pre-stellar cores, which are the initial conditions in some theories of massive star formation. A gas-phase chemical reaction network is applied to MHD simulations, with a focus on predicting the level of deuteration of key diagnostic species that are widely used in observational searches for such cores. We show how the abundances and kinematics of N_2D^+ and N_2H^+ can help disentangle the chemodynamical history of massive cores. Next we examine the formation of populations of cores from colliding and non-colliding giant molecular clouds (GMCs). We begin by carrying out high resolution MHD simulations to examine how core properties, especially the core mass function (CMF), are influenced by the dynamics of the GMCs. Synthetic observations of the simulated clouds are derived to enable a more direct comparison with observed CMFs. We then use a gas-grain chemical network to follow the evolution of key gas- and ice-phase species in these GMCs. One application is a study of the influence of the cosmic ray ionization rate on the abundances of CO, HCO^+ and N_2H^+ in the colliding and non-colliding clouds and how observations of these species can help measure this key environmental property. Associated with the release of our astrochemical modeling tool, Naunet, we also discuss the computational performance of chemodynamical simulations and summarize methods to further improve their efficiency.

Keywords: ISM:clouds, stars:formation, astrochemistry, magnetohydrodynamics, methods:numerical

List of Publications

This thesis is based on the following publications:

[A] **Chia-Jung Hsu**, Jonathan C. Tan, Matthew D. Goodson, Paola Caselli, Bastian Körtgen, and Yu Cheng, "Deuterium chemodynamics of massive prestellar cores". *MNRAS*, vol. 502, 2021. doi:10.1093/mnras/staa4031.

[B] **Chia-Jung Hsu**, Jonathan C. Tan, Duncan Christie, Yu Cheng, and Theo J. O'Neill, "GMC Collisions As Triggers of Star Formation. VIII. The Core Mass Function". Accepted to MNRAS.

[C] **Chia-Jung Hsu**, Jonathan C. Tan, Jonathan Holdship, Duo Xu, Serena Viti and Benjamin Wu, "GMC Collisions As Triggers of Star Formation. IX. The Core Mass Function". Manuscript intended for submission to MNRAS.

Other publications by the author, not included in this thesis, are:

[D] N. Entekhabi, J. C Tan, G. Cosentino, **C.-J. Hsu**, P. Caselli, C. Walsh, W. Lim, J. D. Henshaw, A. T. Barnes, F. Fontani, I. Jiménez-Serra, "Astrochemical modelling of infrared dark clouds". *A&A*, vol. 662, 2022. doi:10.1051/0004-6361/202142601.

[E] Arturo Cevallos Soto, Jonathan C. Tan, Xiao Hu, **Chia-Jung Hsu**, Catherine Walsh, "Inside-out planet formation - VII. Astrochemical models of protoplanetary discs and implications for planetary compositions". *MNRAS* vol. 517, 2022. doi:10.1093/mnras/stac2650.

[F] Duo Xu, Jonathan C. Tan, Xiao Hu, **Chia-Jung Hsu**, Ye Zhu, "Denoising Diffusion Probabilistic Models to Predict the Density of Molecular Clouds". *Accepted to ApJ.*

Acknowledgments

First and foremost, I want to thank my supervisor, Jonathan Tan, for his guidance, support and patience during my PhD. He gave me a special chance to study astronomy and astrochemistry in Sweden and work with many wonderful collaborators. His enthusiasm for science and insightful suggestions also lead me to overcome the research challenge and accomplish things step by step. I also want to thank Susanne Aalto for being my examiner, Jouni Kainulainen for being my assistant supervisor, Vincent Desmaris for being my study leader, and Matthias Maercker for being a kind manager. I can feel your care for my mental health. I also want to thank many group members and collaborators, Giuliana Cosentino, Rubén Fedriani, Prasanta Gorai, Joseph Armstrong, Maya Petkova, Brandt Gaches, Paola Caselli, Serena Viti, Matthew Goodson, Jonathan Holdship, Yao-Lun Yang. You taught me a lot of professional knowledge and experiences. I also want to thank Jasmine Nilsson for helping deal with much paperwork.

I would like to thank all the colleagues I met in AoP Division, especially Andri Spilker, Juan Farias, Sandra Treviño Morales, Chi-Yan Law, Sara Piras, Kyoko Onishi, Mamiko Sato, Iskra Georgieva, Jean-Baptiste Jolly, Jasbir Singh, Vieri Cammelli and many others. You make AoP a wonderful working environment and I really enjoy the time we share together in classes, parks, bars, badminton courts, etc. I also want to thank my Taiwanese friends, Feng-i Tai, Angela Huang, Pi-Fang Lin and many others I met in Gothenburg. You shared a lot of experiences to help me live in Sweden.

Last but not least, I want to thank my family for their support and encouragement. Without your support, I could not even start my study.

Acronyms

CMF:	Core Mass Function
CR:	Cosmic Ray
GMC:	Giant Molecular Cloud
IMF:	Initial Mass Function
IRDC:	Infrared Dark Cloud
ISM:	Interstellar Medium
MHD:	Magnetohydrodynamics
PSC:	Prestellar Core

Contents

Part I

Overview

CHAPTER 1

Introduction

1.1 Introduction

Stars are the most fundamental luminous objects and dominant sources of energy in the universe. However, many questions concerning the star formation process are still under debate. One of the most important of these is: what is the formation mechanism of high-mass stars, i.e., those with masses $> 8\,M_{\odot}$ (e.g., Tan et al., 2014)? Although astrophysicists have a paradigm to explain the formation of low-mass stars (e.g., Shu et al., 1987; Kennicutt & Evans, 2012), such a consensus for massive stars has not yet been reached (e.g, Kahn, 1974; Beuther et al., 2006). A related question is: what processes initiate and regulate the birth of star clusters? Most stars, including massive ones, are thought to form in clusters, so answering this question will also enable a deeper understanding of the stellar initial mass function and the global star formation activity and thus the evolution of galaxies (e.g., Tan et al., 2014; Offner et al., 2014).

Several theories have been proposed to describe massive star formation. Among these, the Turbulent Core Accretion (TCA) model (McKee & Tan, 2003) and the Competitive Accretion model (Bonnell et al., 2001) are the two

main candidates. In short, the TCA model proposes that massive stars form through a mechanism that is a scaled-up version of the process that leads to the birth of low-mass stars. In this scenario, a massive star forms from the collapse of an approximately monolithic massive prestellar core embedded in a molecular "clump" environment. Alternatively, Competitive Accretion suggests that massive stars emerge from a protocluster population of initially low-mass progenitors that feed on the material of the clump. These progenitors steal the clump material from each other, i.e., hence the term "competitive" accretion. As a result, only a small fraction of the progenitors grow into massive stars. This gives rise to a stellar cluster in which both low- and high-mass objects are present. This has implications that extend further than simply the question of how massive stars form. Indeed, while in the Competitive Accretion Model, stars are naturally born in clusters, this is not the case for the TCA model. In addition, the TCA model implies a certain similarity or correlation between the pre-stellar Core Mass Function (CMF) and the stellar Initial Mass Function (IMF), modulated by a core-to-star formation efficiency (e.g., Tan et al., 2014).

On a larger scale, "clumps" are embedded in giant molecular clouds (GMCs) and are the objects leading to the formation of star clusters (Williams et al., 2000; Bergin & Tafalla, 2007; Tan et al., 2014). How clump gas condenses in GMCs is then another question. Collisions between GMCs are a possible mechanism for this, since the process involves supersonic shocks that compress gas on the scales of the contact zones between the clouds. Depending on the level of compression and the fragmentation properties of the magnetised gas, the mechanism may also form massive prestellar cores and trigger the formation of massive stars. Examining the CMFs and stellar IMFs in simulations of this process and comparing to observed systems may allow a test of this model.

Emissions at millimetre wavelengths from molecular rotational transitions provide astronomers a way to identify structures and kinematics in GMCs, clumps and cores. The dynamics inferred from their signals can also help us detect the signatures coming from cloud collision events. At the same time, the chemical abundances probed by the emission lines of each species allow us to investigate the local properties of the structures. In order to best interpret observational results on molecular abundances, it is crucial to have a clear theoretical understanding of the chemical processes that lead to the

production/destruction of each species. The requirement brings us to the topic of astrochemistry.

In the last decades, astrochemists have built a variety of sophisticated models to investigate the chemical evolution of molecular species under the physical conditions typically observed in the interstellar medium (ISM). Most early implementations of these models did not consider any spatial distribution, i.e., being single point models, where the coupled rate equations for various chemical reactions are solved for a given physical condition, i.e., density, temperature, radiation field, cosmic ray ionization rate. However, to model global systems of GMCs, clumps and cores, which are increasingly well-resolved by improving telescope facilities, one needs to follow the chemical evolution in a more general way, i.e., following effects of spatial and temporal variation, including the effects of advective flows. To model the interaction between gas dynamics and chemistry, we need to construct chemodynamical simulations by embedding the astrochemical models into hydrodynamic simulations.

In this thesis, we have developed methods to implement such simulations, including a framework to handle astrochemical models in multiple formats and improve their performance. We have then carried out a series of chemodynamical simulations to study the chemical evolution in the ISM, especially focusing on massive prestellar cores and colliding GMCs. The primary aim is to explore the astrochemical signatures of these targets. However, we have also used our simulations to study physical properties, especially the influence of different levels of magnetisation on cloud structures, such as the CMF. We have made numerous comparisons of our physical and chemical results with observational studies of molecular clouds. Such comparisons can help us constrain the processes that are shaping star formation activity in the Galaxy, including the influence of key environmental parameters, such as colliding or non-colliding GMCs and global cosmic ray ionization rates.

1.2 Thesis outline

In Chapter 2, we review the basic properties of molecular clouds and the star formation process. Chapter 3 introduces our astrochemical modeling methods. The computational tool we have developed to build the chemodynamics simulations will be introduced in Chapter 4. Chapter 5 introduces the appended papers and Chapter 6 describes future work.

CHAPTER 2

Interstellar Medium and Star Formation

The interstellar medium (ISM) is not only the nursery but also the graveyard of stars. It supplies the materials to form new stars and recycles the remnants from the dead stars. It is also shaped by radiative and mechanical feedback from stars. To study star formation, we need to understand the role of the ISM.

2.1 Interstellar Medium

The composition of the ISM is complex. Its composition can be separated into gas, dust, radiation, cosmic rays and magnetic fields. The global composition of the ISM changes as stars form and evolve. Figure 2.1 illustrates the cycle between the interstellar medium and star formation. Stars have different influences, depending on whether they are massive ($> 8M_{\odot}$) or Sun-like (i.e., low-mass). Massive stars are hot, bright, and have short lifetimes. They forge heavy metals inside their cores. At the end of their lives, they explode as supernovae and spread these metals into the ISM and thus change its composition. Low-mass stars like our Sun do not generally create heavy elements beyond oxygen and typically will not end their lives in supernova explosions.

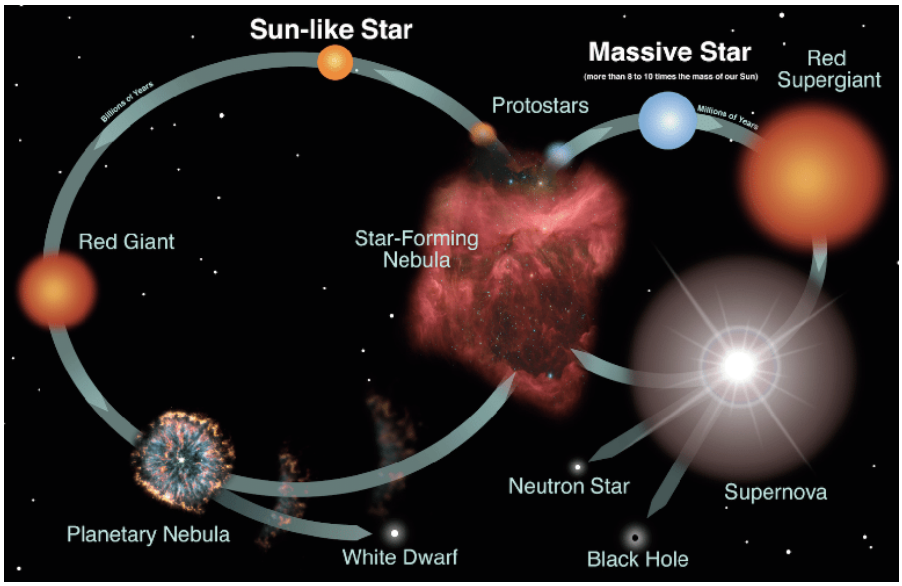

Figure 2.1: Illustration of the cycles of stellar evolution and their influence on the interstellar medium. (Credit: NASA/JPL, Astronomical Society of the Pacific)

However, they may return dust to the ISM during the asymptotic giant branch (AGB) phase. In addition to creating and returning chemical elements, stars also create radiative and mechanical feedback, i.e., in the form of energetic photons, stellar winds and supernova explosions, to shape the ISM. These changes in composition and feedback can be crucial to the formation of the next generation of stars.

It is common to describe the ISM in terms of different phases depending on its composition (e.g. Draine, 2011). In the three-phase model proposed by McKee & Ostriker (1977), the ISM is divided into a hot ionized medium, a warm medium (including warm ionized medium and warm neutral medium), and a cold neutral medium. The hot ionized medium has temperatures $\gtrsim 10^5$ K and is mostly composed of collisionally ionized hydrogen at low density $\sim 10^{-3}$ cm^{-3}. The warm ionized medium phase has a temperature $\sim 10^4$ K and densities in the range from 0.1 to 10^4 cm^{-3}. The H is kept mostly ionized by photoionization from extreme ultraviolet (EUV) photons produced by high-

mass stars. The warm neutral medium phase has a similar temperature, but it has atomic hydrogen as the main composition at a density $\sim 0.1\,\mathrm{cm}^{-3}$. In the cold phase, the composition starts as atomic hydrogen, but H_2 molecules can also form mediated via reactions on the surfaces of dust grains.

The dense molecular phase is also referred to as molecular clouds or dark clouds, reflecting the fact that they have high opacity at optical wavelengths due to their dust content and H is mainly in molecular form. The capability of dust to absorb light and shield the exterior far ultraviolet (FUV) radiation field reduces the destruction rate of H_2 and CO molecules. In addition, the common molecules, especially H_2 and CO, can also self-shield themselves from the exterior light. As a result of shielding, heating by radiation is reduced and low temperatures of around 10 to 50 K are reached. CO, having a permanent dipole moment, exhibits strong rotational transitions and the resulting line emission is one of the main ways to study the properties of molecular clouds. A range of densities are inferred, i.e., in terms of the number density of H nuclei, n_H, molecular clouds are seen to have $n_\mathrm{H} \gtrsim 10^2\,\mathrm{cm}^{-3}$ (Solomon et al., 1987; Roman-Duval et al., 2010) on large scales of giant molecular clouds (GMCs). These GMCs are the sites of most star formation in our Galaxy and other galaxies (McKee & Ostriker, 2007; Kennicutt & Evans, 2012).

The mass of molecular clouds varies over a wide range, e.g., from $\sim 10^2$ to $\sim 10^7\,M_\odot$ (McKee & Ostriker, 2007; Kennicutt & Evans, 2012; Dobbs et al., 2014), with GMCs defined as having a mass higher than $10^4\,M_\odot$. The internal structures of moelcular clouds are inhomogeneous. A clump is defined as a velocity-coherent structure that may form a star cluster, while a core is a self-gravitating structure that forms a single rotationally supported disk to yield either a single star or small multiple system via disk fragmentation (Williams et al., 2000; Bergin & Tafalla, 2007; Tan et al., 2014). Typically, clumps have densities $n_\mathrm{H} \gtrsim 10^3\,\mathrm{cm}^{-3}$ and cores have densities $n_\mathrm{H} \gtrsim 10^4\,\mathrm{cm}^{-3}$ (Bergin & Tafalla, 2007). A prestellar core (PSC) refers to a core in a stage just before it forms a star, while a protostellar core is the stage when a protostar, i.e., an object of stellar density, has already formed, but is still accreting.

2.2 Star Formation Stages

Many aspects of star formation are still under debate, but there is a consensus picture for the formation of low-mass stars. These stars are thought to form

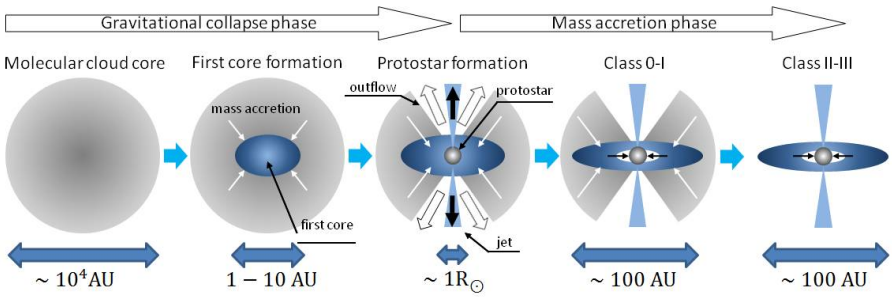

Figure 2.2: Illustration of low-mass star formation by Core Accretion. (Credit: Yusuke Tsukamoto)

from prestellar cores residing in molecular clouds with the following stages (e.g. Shu et al., 1987; Kennicutt & Evans, 2012) (see also Figure 2.2):

- Prestellar Core (PSC): a dense, self-gravitating, centrally-concentrated substructure that condenses out of the ambient molecular clump. PSCs typically exhibit infall motions.
- Protostellar Core: once the internal pressure cannot support against gravitational force, the central region of the prestellar core collapses and forms a "first core" that is approximately hydrostatic equilibrium, but still undergoing accretion. The gravitational energy heats up the gas in this core. Once the temperature reaches about 2,000 K, molecular hydrogen is dissociated, leading to further collapse to a true protostellar structure. Continued accretion is occurring from the infall envelope and a rotationally supported disk. Magnetic fields in the rotating protostar and disk launch bipolar protostellar outflows that begin to clear cavities above and below the disk. The main accretion phase when most of the mass of the star is built up is thought to be in the highly embedded "Class 0" phase.
- Envelope Dispersal: During the "Class I" phase the infall envelope gradually dissipates, partly due to accretion to the central source and partly due to the mechanical feedback from the protostellar outflow. It is possible that the first stages of planet formation occur already in this phase.
- Disk Dispersal: Once the envelope is dispersed, the young stellar object

(YSO) is described as being in the "Class II" phase, i.e., still retaining a circumstellar disk of gas and dust. The disk gradually dissipates, by accretion, outflow and planet formation to eventually leave a diskless "Class III" source.

2.3 Massive Star Formation

Unlike the formation of low-mass stars, the formation mechanism of massive stars cannot be simply explained by the procedure described above. For example, a massive prestellar core may be much more prone to fragmentation into lower-mass stars if it lacks sufficient internal pressure support. In addition, a massive protostar releases much stronger radiative and mechanical feedback. Strong radiation pressure acting on dust gas may stop the whole accretion process and prevent formation of stars $\gtrsim 10\,M_{\odot}$ (Kahn, 1974; Beuther et al., 2006). To solve these problems, several theories, including the Turbulent Core Accretion (TCA) model and the Competitive Accretion model, have been proposed as possible scenarios.

The TCA model (McKee & Tan, 2003) is a scaled-up version of low-mass star formation theory based on Core Accretion (Shu et al., 1987) (see Figure 2.2). The model proposes that a combination of supersonic turbulence and magnetic fields support massive PSCs against fragmentation and that these then undergo approximately monolithic collapse to a central star-disk system. High accretion rates and disk-mediated accretion mechanism then help massive stars form. The collapse in the model is not necessarily as ordered as in the case of low-mass star formation, especially if there is significant turbulence in the PSC. However, it has been argued that turbulence alone cannot prevent a massive prestellar core from fragmenting, and that stellar feedback or a strong magnetic field may be needed (e.g., Dobbs et al., 2005; Krumholz & McKee, 2008; Myers et al., 2013; Tan et al., 2014; Kong et al., 2018).

In contrast, the Competitive Accretion model of Bonnell et al. (2001) proposes that large numbers of low-mass stars form in a protocluster clump and then accreting chaotically by Bondi-Hoyle accretion of gas supplied by the collapsing clump. A small fraction of the stars eventually become massive stars. In this mechanism, the final mass is decided by the gas fed by the clump instead of being decided by the PSC. As a consequence, the model explains why massive stars are usually found in star clusters, but it is hard to explain

examples of isolated massive stars. In addition, Competitive Accretion tends to form massive stars more slowly (e.g., in $\sim 1\,\mathrm{Myr}$) and with lower accretion rates (e.g., $\sim$ few $\times 10^{-5}\,M_\odot\,\mathrm{yr}^{-1}$) than the TCA model. Such low accretion rates may make it difficult to reach a mass higher than 10 $M_\odot$ as radiation pressure acting on dusty gas can inhibit the Bondi-Hoyle accretion (Tan et al., 2014).

A major distinction between the two scenarios is the existence of massive, coherent PSCs. Hence, one way to discern between the two theories would be to prove the existence of such objects. However, massive PSCs, like massive stars themselves, are relatively rare and tend to form far from the Sun. The PSCs would be cold objects and so relatively weak emitters of dust continuum emission that may be hard to separate out from the surrounding clump. This motivates an investigation on whether there are good astrochemical tracers of PSCs that could be used to identify such objects, which will be further explained in Section 2.7.

2.4 Stellar Initial Mass Function

The stellar initial mass function (IMF) is the probability distribution function (PDF) of stellar masses arising from the star formation process. Salpeter (1955) introduced a power-law description of the stellar IMF:

$$\frac{dN}{d\log M} \propto M^{-\alpha}, \tag{2.1}$$

where $\alpha \simeq 1.35$ was derived for stars between 0.4 $M_\odot$ and 10 $M_\odot$. Although more recent studies proposed a variety of corrections to the function at the low-mass end (e.g., Kroupa et al., 2001; Chabrier, 2003), the above value of α remains a standard value to describe the power-law tail of IMF in the range of $m_* > 1\,M_\odot$ (see Figure 2.3). The universality and origin of IMF have been debated for many years (e.g., Bastian et al., 2010; Offner et al., 2014). One of the main open questions is whether the stellar IMF results from the core mass function (CMF), which is the equivalent PDF of dense, pre-stellar cores (e.g., Offner et al., 2014).

In the context of the Core Accretion Model, it is expected that there is a direct correspondence between the CMF and IMF, but modulated by a core to star formation efficiency, which may be mass dependent (e.g. Padoan

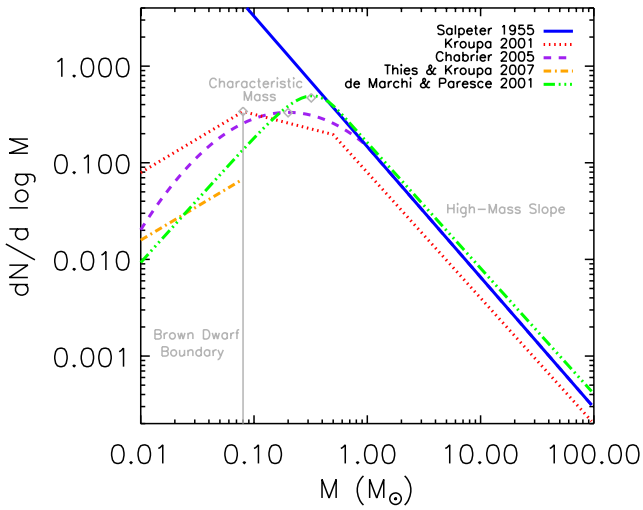

Figure 2.3: Examples of several initial mass functions (Credit: Offner et al., 2014).

& Nordlund, 2002; Hennebelle & Chabrier, 2008; Tan et al., 2014). There is some observational support for a similarity between the CMF and IMF, which supports this idea (e.g., Alves et al., 2007; Ohashi et al., 2016). However, from the perspective of the Competitive Accretion Model, the IMF is an outcome of the dynamical evolution (e.g., Bonnell et al., 2001; Bate et al., 2003) and the similarity between the CMF and IMF is coincidental.

2.5 Cloud-Cloud Collisions

Although the Turbulent Core Accretion and Competitive Accretion models give possible answers to the question of massive star and star cluster formation, these models do not address the origin of clumps themselves. Among a variety of different possible mechanisms, e.g., regulation by turbulence, magnetic fields, feedback, spiral arms, converging atomic flows (e.g., see review by McKee & Ostriker, 2007), collisions between giant molecular clouds (GMCs) have been proposed as a promising way to form dense clumps and trigger for-

mation of massive stars and star clusters (e.g., Scoville et al., 1986). Galactic shear driven collisions have been proposed to happen frequently enough to dominate the star formation rate, which would then provide a natural explanation of the dynamical Kennicutt-Schmidt relation (Tan, 2000). Numerical simulations works have indeed found that this type of event can happen frequently, occurring in less than 20% of orbital time (e.g., Tasker & Tan, 2009; Dobbs et al., 2015; Li et al., 2018).

Observational studies have also revealed the occurrence of cloud collisions and their role in triggering star formation. Fukui et al. (2021) listed more than 50 high-mass star-forming regions that show evidence for cloud collision signatures. In these studies, the occurrence of a cloud collision can be identified by: (1) a spatially complementary distribution with displacement; (2) U-shape morphology of the gas; and (3) the "bridge effect" in a position-velocity diagram of CO emission lines (e.g., Galván-Madrid et al., 2010; Nakamura et al., 2012; Fukui et al., 2018; Dewangan, 2022). In addition, Jiménez-Serra et al. (2010) and Cosentino et al. (2018) proposed that the emission from shock tracers, particularly SiO, can indicate the occurrence of cloud collisions and found the signatures in several infrared dark clouds (IRDCs). However, similar chemical signatures have been suggested to also appear in the process of hierarchical gravitational collapse or feedback-driven flows and thus not be a unique signature of the GMC collision process (e.g., Chevance et al., 2020).

2.6 Physical Processes

Star formation is a complex dynamical process involving a multitude of different physical effects. In the stages from molecular clouds to collapsing cores, the roles of self-gravity, turbulence and magnetic fields are thought to be particularly important (e.g., Hennebelle et al., 2011).

Gravity

As a long-range attractive force, gravity is essential for the concentration of mass into stars, i.e., star formation. A simple criterion to estimate whether a gas cloud is unstable with respect to thermal pressure support is the Jeans analysis, from which the Jeans length describes the minimum scale of unstable

modes:

$$\lambda_J = \left(\frac{\pi c_s^2}{G\rho}\right)^{1/2}, \tag{2.2}$$

where $c_s = (\gamma kT/\mu m_{\rm H})^{1/2}$ is the sound speed and ρ is the density of the medium. For a spherical, uniform density cloud that is gravitationally unstable, the free-fall time is a characteristic timescale of collapse, defined by:

$$t_{\rm ff} = \sqrt{\frac{3\pi}{32G\rho}}. \tag{2.3}$$

Note, this assumes negligible internal pressure support resists collapse, so is the minimum time for collapse of more realistic systems that experience some internal pressure support.

A way to measure the importance of gravity in a system is via the virial parameter, which is derived from the virial theorem. From classical mechanics, a system of particles is in virial equilibrium if the kinetic energy $E_{\rm KE}$ and the gravitational potential energy E_G satisfy the relationship:

$$2E_{\rm KE} + E_G = 0. \tag{2.4}$$

In the case of spherical clouds/clumps/cores of mass M and radius R, the internal kinetic energy, $E_{\rm KE}$, is related to the 1-D velocity dispersion, σ via $E_{\rm KE} = (3/2)M\sigma^2$. The virial parameter, $\alpha_{\rm vir}$, is defined by

$$\alpha_{\rm vir} = 5\sigma^2 R/(GM) = 2aE_{\rm KE}/E_G, \tag{2.5}$$

where a is the ratio of gravitational energy, E_G, to that of a uniform sphere, $3GM^2/(5R)$ (Bertoldi & McKee, 1992). Although astronomical objects are not in practice of uniform density and contain thermal and magnetic field energy, the virial parameter provides a simple way to assess, approximately, whether a system is gravitationally bounded ($\alpha_{\rm vir} < 2$). A system is said to be subvirial if $\alpha_{\rm vir} < 1$ and supervirial if $\alpha_{\rm vir} > 1$, although one should remember that the virial equilibrium value of $\alpha_{\rm vir}$ varies depending on the precise internal density structure, degree of elongation, amount of large-scale $B-$field support and intensity of surface pressure.

Turbulence

In fluid dynamics, turbulence is the chaotic fluid motion derived from an irregular velocity field. The occurrence of turbulence is a competition between inertial force and viscous force and it can be characterized by the Reynolds number:

$$\mathrm{Re} \sim \frac{Lv}{\nu}, \tag{2.6}$$

where L, v, and ν are the characteristic length, characteristic velocity and viscosity of the fluid. If $\mathrm{Re} \lesssim 1$, the viscous force dominates the motion and the fluid follows a laminar flow. In the case of $\mathrm{Re} \gg 1$, the inertial force dominates the motion and turbulence occurs. The interstellar medium typically has $\mathrm{Re} \sim 10^9$ and is highly turbulent. The turbulence in molecular clouds may be important in providing support against gravitational collapse.

Although turbulence involves irregular motion, it still has some well-defined statistical properties, particularly in the power spectrum, which can be derived from the Fourier transform of the velocity field, $\mathbf{v}(\mathbf{k})$, according to:

$$E(\mathbf{k}) = |\mathbf{v}(\mathbf{k})|^2, \tag{2.7}$$

where $\mathbf{k}$ is the wave vector. The equation can be reduced to:

$$E(k) = 4\pi |v(k)|^2, \tag{2.8}$$

if the turbulence is isotropic. Kolmogorov turbulence is the case for a subsonic incompressible fluid. It has power spectrum $E(k) \propto k^{-5/3}$. For a supersonic compressible fluid, the shocks result in a power spectrum of $E(k) \propto k^{-2}$, which is known as Burger's turbulence.

Magnetic Fields

Unlike turbulence, magnetic fields contribute to the pressure support in a gas cloud in a way that cannot be directly seen from the gas motions. For a cloud/clump/core that is threaded by a given magnetic flux, Φ, it will be able to collapse under gravity if its mass is greater than the magnetic critical mass (Mouschovias & Spitzer, L., 1976):

$$M_\Phi = \Phi/(2\pi G^{1/2}). \tag{2.9}$$

The ratio of the actual cloud mass to M_Φ then defines a dimensionless parameter:

$$\mu_\Phi = \frac{M}{M_\Phi} = \frac{2\pi G^{1/2} M}{\Phi}. \tag{2.10}$$

If $\mu_\Phi > 1$, then the cloud is magnetically supercritical and the $B-$fields cannot prevent collapse. Alternatively, if $\mu_\Phi < 1$, then the cloud is magnetically subcritical and collapse to a star is only possible if some magnetic flux is lost from the mass, e.g., via ambipolar diffusion.

2.7 Tracing Star-Forming Regions

Star formation happens inside molecular clouds, but these regions are typically highly opaque at optical and near-infrared (NIR) wavelengths where most young stars have the peak of their photospheric emission. In addition, the protostellar and earlier phases involve cooler temperature material that emits at longer wavelengths. For these reasons, most studies of star formation, especially its early stages, generally involve observations at longer wavelengths, e.g., in the mid-infrared (MIR), far-infrared (FIR) or sub-mm/mm/radio regimes. Such wavelengths are sensitive to the thermal emission from dusty gas in molecular clouds from temperatures ~ 10 K of PSCs to the several hundred K temperatures of massive protostellar disks and infall envelopes. Due to the influence of the Earth's atmosphere, especially its water vapor content, observations in the MIR and FIR can often require space-based telescopes, such as Spitzer, Herschel and JWST.

In the densest regions, the dust extinction is so high that even MIR light is obscured. These sites are recognized as infrared dark clouds (IRDCs) (Egan et al., 1998; Simon et al., 2006). Previous studies have shown that these clouds are dense ($n_{\rm H} \gtrsim 10^4$ cm^{-3}) and cold (< 25 K) and can be the birthplace of massive stars (e.g., Butler & Tan, 2012). Many studies of IRDCs have been carried out by observation of molecular rotational line emission at sub-mm wavelengths, where the clouds are generally optically thin. However, while molecular hydrogen is the most abundant species inside GMCs or IRDCs, it is not easy to be observed. Its radiative inefficiency due to the lack of a permanent dipole moment and the high energy gap between its rotational states makes it hard to be excited in the low-temperature environments typical of GMCs and IRDCs. Therefore, CO has been used as the main proxy to

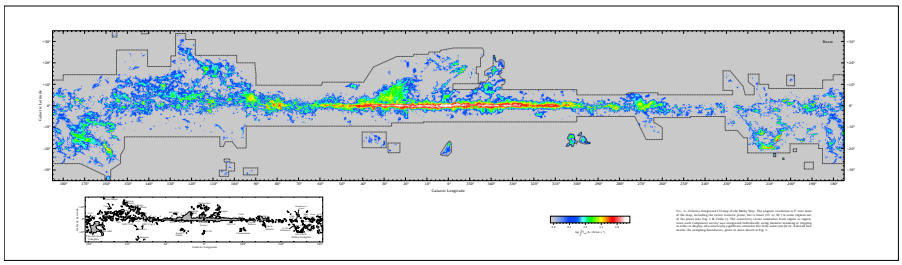

Figure 2.4: CO maps of the Milky Way (Dame et al., 2001).

trace the molecular gas because it is the second most abundant molecule and can be excited at low temperatures. Figure 2.4 shows an example of how CO traces molecular gas, including GMCs, in our Milky Way (Dame et al., 2001). However, as will be explored further in this thesis, at cold temperatures ($\lesssim 20\,\mathrm{K}$) and under dense conditions relevant to IRDCs, CO freezes out from the gas phase to form CO ice mantles on dust grains. Thus, other chemical species, such as N_2H^+, can be important to trace molecular gas in these environments.

If the main mechanism to excite molecules is collisions, the density is crucial to determine whether such collisions are frequent enough to populate upper state levels sufficiently for strong emission lines to be seen. For an emission line from a two-level system and optically thin, this critical density is determined by:

$$n_{\mathrm{crit}} = \frac{A_{\mathrm{ul}}}{k_{\mathrm{ul}}}, \tag{2.11}$$

where A_{ul} and k_{ul} are the Einstein A coefficient and collisional de-excitation rate (e.g., Krumholz, 2015). If a particular molecule has a higher critical density, then it will tend to trace regions with densities similar to this critical value. For example, the $C^{18}O$(1-0) rotational transition has a critical density of about 2,000 cm^{-3}, while the HCO^+(1-0) transition has a critical density around 2×10^5 cm^{-3} (van der Tak et al., 2020). Therefore, HCO^+, if present at sufficient abundance, is able to tell us more information about relatively denser regions, compared to $C^{18}O$(1-0).

CHAPTER 3

Astrochemical Models

Astrochemistry is the study of the formation, destruction, and excitation of molecules in astronomical environments and their influence on the structure, dynamics, and evolution of astronomical objects (Dalgarno, 2008). In accordance with the definition, we understand that astrochemistry involves a variety of aspects. First, astronomical environments decide the evolution of chemical species in space. It also means that the astronomical environment can be interpreted from the chemical abundances derived from observations. In addition, the chemical species formed in space also influence the evolution of the ISM material they reside in several ways. For example, a direct influence is from the thermal energy released or absorbed from the formation or destruction reactions of various species. The energy state transition can also emit or absorb energy from the interstellar radiation field to change the energy content of the objects. Furthermore, chemical processes also influence the ionization fraction of interstellar gas and the movement of these charged particles is coupled with magnetic fields leading to the ability of a cloud to feel magnetic pressure effects, e.g., as a support against gravitational collapse.

The study of astrochemistry involves observations, theoretical models, and experiments. Theoretical models can be further broken down into quan-

tum mechanical calculations and simulations, Monte Carlo simulations (e.g., Vasyunin & Herbst, 2013), and rate equation simulations, from microscopic to macroscopic viewpoints. In this thesis, we mainly utilise the rate equation method, which is also the most common way to simulate chemical abundances in space and gives us an easier interface to couple with magneto-hydrodynamic (MHD) simulations (see Chapter 4). Here, we briefly introduce how the main interstellar medium components affect astrochemical processes.

3.1 Interstellar Medium Chemistry

The uniqueness of astrochemistry is from the specialty of space environments. The compositions of the ISM, including gas, dust, radiation, cosmic ray and magnetic field, play different roles in astrochemistry.

Gas

One of the main reasons making astrochemistry different from chemistry on Earth is the gas density. In interstellar space, the gas density is far lower than in terrestrial environments. This causes molecules to have low rates of collisional interactions leading to long timescales for certain reactions to occur. In addition, hydrogen is far more abundant than all other elements, with the next most abundant chemically important species, i.e., C and O, being present at levels of one to a few $\times 10^{-4}$ compared to H.

Dust

Dust grains play a crucial role in astrochemistry. Dust grains typically have a bulk composed of carbonaceous and silicate compounds (e.g., Tielens, 2005). Figure 3.1 shows an example of an interplanetary dust particle captured by an aircraft and indicates how dust may look in interstellar space. Grain sizes are inferred to be distributed from 0.01 to 1 μm, depending on the cloud environment (e.g., Schulz, 2012) so that they scatter or absorb UV and optical photons, but become transparent in the far-infrared. This absorption is important to the formation of molecules as it prevents the UV radiation dissociating the molecules so that they can have a long lifetime in the clouds. The amount of extinction along a given path length is typically parameterized in terms of the magnitudes of visual extinction, A_V. For local ISM dust to

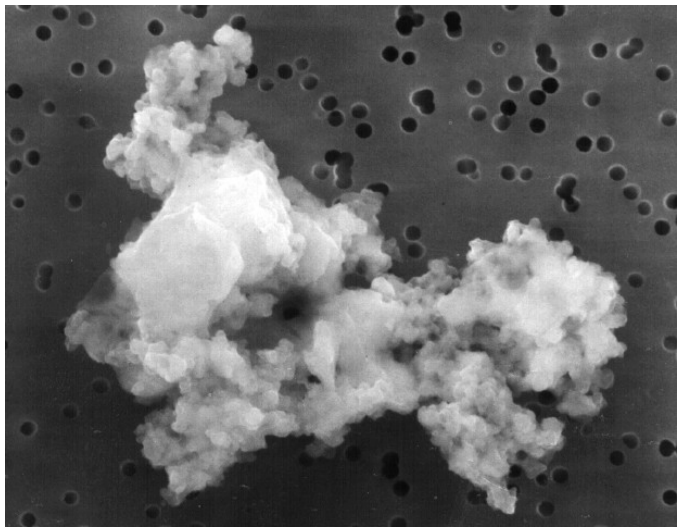

Figure 3.1: A piece of interplanetary dust caught by a high-flying U2-type aircraft. (Credit: NASA)

gas properties, this is proportional to the total column density of H nuclei, N_{H}, in a relation of $N_{\mathrm{H}} \simeq 1.8 \times 10^{21} (A_V/\mathrm{mag})\,\mathrm{cm}^{-2}$.

Dust is also crucial for its ability to provide surfaces where molecules can stick and provide sites for them to react. These two processes refer to depletion (or freeze-out) and surface reactions. Some exothermic reactions cannot happen without dust absorbing the excess heat. An important example is the formation of H_2. In addition, various complex organic molecules also cannot form efficiently unless dust provides a place for various larger molecules and radicals to meet.

UV Radiation

Stars, especially massive stars, can be strong emitters of UV radiation. The photons having energy higher than 13.6 eV are easily absorbed by atomic hydrogen. However, UV radiation with energy lower than 13.6 eV (wavelength longer than 912 Å) can still penetrate diffuse gas and destroy molecules. The strength of the UV radiation is often described with a scaling factor G_0, which indicates the ratio to the interstellar radiation field (ISRF) to that

of a characteristic value in the local ISM known as a Habing field (Habing, 1968; Draine, 1978; Mathis et al., 1983). UV and optical photons are readily adsorbed by dust, thus heating the grains. Some of this heat energy can be transferred to the gas. Another part is re-radiated as infrared light, which has a higher chance of escaping from the region. As a result of this heating, starless molecular clouds tend to have a higher temperature, ~ 50 K, on their boundaries and become colder inside, down to ~ 10 K, as more UV photons are shielded.

Cosmic Rays

Cosmic rays are high-energy particles, i.e., with energies $\gtrsim$ MeV. Depending on their energy, cosmic rays can penetrate more deeply into dense molecular clouds and ionize chemical species, especially leading to the formation of H_3^+, which then initiates a whole sequence of ion-molecule reactions. The cosmic ray (primary) ionization rate is denoted by ζ, with typical local ISM values estimated to be $\sim 10^{-17}$ to $10^{-16}\,\mathrm{s}^{-1}$. H_2 molecules can also be excited by cosmic rays and generate a local UV radiation field (Prasad & Tarafdar, 1983; Shen et al., 2004). Cosmic rays and their induced local UV radiation field also can play important role in the non-thermal desorption of molecules from the dust surfaces back to the gas phase **(e.g., Hasegawa & Herbst, 1993; Wakelam et al., 2021).**

3.2 Rate Equation Approach

The rate equation approach is one of the most common methods used to study astrochemistry. In this approach, each species is described with an ordinary differential equation (ODE), and the combination of these equations forms a system. To understand the evolution of species, we have to solve the ODE system. In this kind of system, the left-hand side (LHS) of the equations is the time differential term of each species, i.e., dn_i/dt, and the right-hand side (RHS) is the function used to calculate the rates depending on the current state, which is usually denoted as $f_i(\mathbf{n}, t)$. The chemical network/model then provides the reaction rate to determine the $f_i(\mathbf{n}, t)$. A Jacobian matrix, J, can also be derived from the equations $dn_i/dt = f_i(\mathbf{n}, t)$ in the form of $dn_i/dt = J \cdot \mathbf{n}$, where $J_{ij} = \partial f_i(\mathbf{n}, t)/\partial n_j$. The Jacobian matrix counts the contribution

from each species and is usually used to accelerate the numerical performance.

As mentioned above, material in the ISM can be either in the gas phase or frozen-out onto dust grains. Typically, we use the term "ice-phase" to describe the species on dust grains. The species that stay in different phases are considered as different species when we construct the ODE system, even if their chemical composition is identical. The purpose is to precisely track the state of the species. However, several studies have suggested more phases in the chemical models. For example, a three-phase model is sometimes used to consider relatively active and passive layers on dust grains. The idea has been proposed in Hasegawa & Herbst (1993) because they believe that the species on the dust grains can form multiple layers. The species that stay on top layers are more active to diffuse and react with each other than the bottom layers. The difference of the top layers and bottom layers can be referred to "surface" and "bulk", respectively, and are treated as different species in an ODE system. The surface species can be converted to bulk phase as long as more species stick onto the grain surface and occupy all the space/sites on the surface. The bulk species can also be converted back to the surface phase if the surface is desorbing (e.g. Ruaud et al., 2016).

In a three-phase model, the ODEs of gas-phase species are expressed in the following equation:

$$\begin{aligned}\frac{dn_i}{dt} = &\sum_j \sum_k k_{jk} n_j n_k + \sum_j k_{cr,j} n_j + \sum_j k_{ph,j} n_j + k_{des,i} n_i^s \\ &- \sum_i \sum_j k_{ij} n_i n_j - k_{acc,i} n_i - k_{cr,i} n_i - k_{ph,i} n_i,\end{aligned} \tag{3.1}$$

where n_i is the current abundance of the i-th species and n_i^s is its corresponding surface species, k_{ij} means the reaction rates whose reactants are the i-th and the j-th species, $k_{acc,i}$, $k_{des,i}$, $k_{cr,i}$, $k_{ph,i}$ are the accretion rate, desorption rate, cosmic ray ionization/dissociate rate, and photon ionization/dissociation rate.

Similarly, the evolution of surface species or bulk species can be expressed

in the following equations:

$$\begin{aligned}\frac{dn_i^s}{dt} &= \sum_j \sum_k k_{jk} n_j^s n_k^s + \sum_j k_{cr,j} n_j^s + \sum_j k_{ph,j} n_j^s + k_{acc,i} n_i \\ &- \sum_i \sum_j k_{ij} n_i^s n_j^s - k_{des,i} n_i^s - k_{cr,i} n_i^s - k_{ph,i} n_i^s \\ &+ k_{swap,i}^b n_i^b + \frac{dn_i^b}{dt}|_{b\to s} - k_{swap,i}^s n_i^s + \frac{dn_i^s}{dt}|_{s\to b}\end{aligned} \tag{3.2}$$

$$\begin{aligned}\frac{dn_i^b}{dt} &= \sum_j \sum_k k_{jk} n_j^b n_k^b + \sum_j k_{cr,j} n_j^b + \sum_j k_{ph,j} n_j^b \\ &- \sum_i \sum_j k_{ij} n_i^b n_j^b - k_{cr,i} n_i^b - k_{ph,i} n_i^b \\ &+ k_{swap,i}^s n_i^s + \frac{dn_i^s}{dt}|_{s\to b} - k_{swap,i}^b n_i^b - \frac{dn_i^b}{dt}|_{b\to s},\end{aligned} \tag{3.3}$$

where n_i^b is the corresponding bulk species, and k_{swap} is the swapping rate between surface and bulk states, dn_i/dt is the individual transfer for species between bulk and surface. It reflects the influence of accretion and desorption (e.g. Ruaud et al., 2016). If the three-phase model does not trace the evolution of bulk species, the swapping rate and transfer rate are zero, but the abundance of surface species will multiply a coverage factor to only count the abundances on the top active monolayers (e.g. Hasegawa & Herbst, 1993).

3.3 Chemical Reaction Rates

In the last section, we have explained how to construct an ODE system from the reaction rates. The evaluation of chemical reaction rates is then based on the chemical model. Different models have different ways to evaluate reaction rates. Generally, reactions can be categorized to gas-phase reactions, gas-grain reactions and grain surface reactions. Each of them has different methods to decide the reaction rates. Gas-phase reactions mean the reactions only involve species that are both in the gas phase, but UV photons and CR particles can also be involved. Gas-grain interactions term the reactions happening among species and dust grains, especially the accretion (freeze-out) reactions and multiple desorption mechanisms. UV photons and CR particles can also play

an important role in desorption. Grain-surface reactions specify the reactions happening on dust grain surface and the grain properties, such as the size of the grain and the number of surface sites, are also important factors to determine the reaction rates. A clear review of the reaction rates can be found in Cuppen et al. (2017), but here we briefly introduce how the chemical reaction rates are evaluated.

Gas-Phase Reaction

Gas-phase reactions are the foundation of chemical reaction networks. In the past decades, the astrochemistry community has studied a great variety of gas-phase reactions occurring in space and obtained some ideas about their reaction rates. Most of these gas-phase reactions have been collected into two popular databases, KIDA (Wakelam et al., 2012) and UMIST (McElroy et al., 2013), and astrochemists can build their own networks/models based on these databases by extending the pre-existing gas-phase reactions with their own dust grain models. These networks/models are usually published with astrochemical codes, such as `Nahoon`(Wakelam et al., 2012), `AstroChem`(Maret & Bergin, 2015), `Nautilus`(Ruaud et al., 2016), and `UCLCHEM`(Holdship et al., 2017).

When it comes to calculating the gas-phase reaction rates, these databases further break the reactions into smaller groups. Each group has a formula to determine the reaction and the formulas usually depend on three coefficients: α, β, γ. KIDA and UMIST have different ways to divide up the reactions into smaller groups. However, they still share the same formulae at a certain level.

There are five main formulae used in the KIDA database and these are given in the following list:

- cosmic ray ionization: $k = \alpha\zeta$, where ζ is the cosmic ray ionization rate referring to molecular hydrogen. The formula is applied to direct cosmic-ray-induced reactions.

- photo-dissociation: $k = \alpha e^{-\gamma A_V}$, where A_V is the visual extinction. For the self-shielding species, like H_2, CO and N_2, the reaction rates may be replaced by other functions (e.g., van Dishoeck & Black, 1988) or multiplying another factor to the formula to include such effects (e.g. Visser et al., 2009).

- modified Arrhenius (bimolecular): $k(T) = \alpha(T/300)^{\beta}e^{-\gamma/T}$. Most two-body reactions among gas-phase species are estimated by this formula.
- ionpol1: $k(T) = \alpha\beta(0.62 + 0.4767 \times \gamma(300/T)^{0.5})$. The reaction rate between ions and dipole neutral species at a low temperature.
- ionpol2: $k(T) = \alpha\beta(1 + 0.0967 \times \gamma(300/T)^{0.5} + (300/T) \times \gamma^2/10.526)$. The reaction rate between ions and dipole neutral species at a high temperature.

UMIST also has similar formulae for the first three kinds of reactions. However, it calculates the rates of cosmic-ray-induced photoreactions separately with the formula: $k(T) = \alpha(T/300)^{\beta} \times \gamma/(1-\omega)$, where ω is the dust-grain albedo. In KIDA, this formula was integrated with the formula of cosmic ray ionization by assuming ω is 0.5 and atomic hydrogen is much less than molecular hydrogen, which is valid in dense gas (Wakelam et al., 2012).

Gas-Grain Interaction

The interaction between gas species and dust grains includes accretion and desorption reactions. Accretion also refers as freeze-out or depletion reaction. One of the most common ways to calculate the accretion rate was proposed in Hasegawa et al. (1992):

$$k_{acc,i} = S_i \pi a^2 \langle v_i \rangle n_d, \tag{3.4}$$

where S_i is the sticking coefficient and is usually set to be unity in ISM. Here a is the radius of the dust grain and πa^2 represents the cross-section of the dust grain. A typical value of a is around 0.1 μm. $\langle v_i \rangle = (8k_BT/\pi m_i)^{1/2}$ is the mean thermal velocity of the species and n_d is the number density of dust grains. In another approach, Rawlings et al. (1992) proposed that the accretion rate is:

$$k_{acc,i} = -4.57 \times 10^4 C S_i \pi a^2 n_d (T/m_i)^{1/2}, \tag{3.5}$$

where C is a factor, which is unity for neutral species but $1+(16.71\times10^{-4}/(aT)$ for singly charged positive ions.

Desorption reactions can be contributed by several mechanisms, and they can be separated into thermal desorption and non-thermal desorption. Ther-

mal desorption depends on the dust temperature T_d and the rate is given by (Hasegawa et al., 1992):

$$k_{thd,i} = \nu_{0,i} e^{-E_{b,i}/T_d}, \tag{3.6}$$

where $\nu_{0,i} = (2N_s E_{b,i}/\pi^2 m_i)^{1/2}$ is the characteristic vibrational frequency of each adsorbed species and $E_{b,i}$ is the binding energy of each species. N_s is the surface density of binding sites. For the three-phase models considering active monolayers (e.g., Hasegawa & Herbst, 1993), the rate is modified to:

$$k_{thd,i} = \nu_{0,i} e^{-E_{b,i}/T_d} N_{act} n_s \sigma_d n_d / \sum_j n_j^s, \tag{3.7}$$

where N_{act} is the number of active monolayers and $\sigma_d = 4\pi a^2$ is the surface area of dust grains. This modification can effectively limit the desorption to only act on the top N_{act} layers on the grains, but only valid when $N_{act} \leq n_i^s / \sum_j n_j^s$.

The exact mechanisms inducing non-thermal desorption are still under debate. However, it is believed that UV photons and cosmic rays can contribute to desorption. To model the cosmic-ray-induced desorption, Hasegawa & Herbst (1993) adapted the study of Leger et al. (1985) and assumed that much of this kind of desorption happens when the dust grain is heated up by cosmic rays to around 70 K. With this assumption, the cosmic-ray-induced desorption rate can be simplified to:

$$k_{crd,i} = F_{cr} f(70\mathrm{K}) k_{thd,i}(70\mathrm{K}), \tag{3.8}$$

where F_{cr} is the flux of cosmic rays and usually is set by a ratio to the average cosmic ray ionization rate, ζ. $f(70\mathrm{K})$ is the fraction of time for grains staying around 70 K and was estimated to be $\sim 3.16 \times 10^{-19}$. However, this estimation likely involves a high uncertainty (Roberts et al., 2007; Cuppen et al., 2017). By only considering the number of molecules capable of being desorbed per cosmic ray impact, (Roberts et al., 2007) proposed using the following formula to obtain the cosmic-ray-induced desorption rate:

$$k_{crd,i} = F_{cr} \pi a^2 n_d \phi n_i^s / \sum_j n_j^s. \tag{3.9}$$

For the desorption induced by photons, Tielens & Hagen (1982) proposed the desorption rate to be:

$$k_{phd,i} = F_{\mathrm{UV}} Y_{\mathrm{UV}} \sigma_d, \tag{3.10}$$

where F_{UV} is the flux of photon and Y_{UV} is the photodesorption yield. If active monolayers are considered, $k_{phd,i}$ will also multiply $N_{act} n_s \sigma_d n_d / \sum_j n_j^s$ to confine the reactions to the active monolayers. In Roberts et al. (2007). F_{UV} is substituted with 4875 $\mathrm{cm}^{-2}\mathrm{s}^{-1}$. The value includes the secondary photons induced by cosmic rays.

Roberts et al. (2007) also mentioned another desorption mechanism induced by the formation of molecular hydrogen, due to the energy released in this exothermic reaction. The rate is then estimated by:

$$k_{H2d,i} = \epsilon R_{\mathrm{H2}} n_i^s / \sum_j n_j^s, \tag{3.11}$$

where R_{H2} is the formation rate of molecular hydrogen and is approximated to $3.16 \times 10^{-17} n(\mathrm{H}) n_{\mathrm{H}}$ in the study. Here $n(\mathrm{H})$ and n_{H} are the number density of atomic hydrogen and the number density of total H nuclei.

By considering exothermic reactions occurring on grain surfaces, Garrod et al. (2007) also proposed the idea of reactive desorption. If the surface reactions (especially from the Langmuir-Hinshelwood mechanism, see Section 3.3) are exothermic and have only one product, this mechanism assumes that there is a probability to eject the single product back to the gas phase.

In general, the binding energies of species play an important role to determine the desorption rates. In the model of Hasegawa et al. (1992) and Hasegawa & Herbst (1993), the binding energy term appears in the exponent. In contrast, the models based on Roberts et al. (2007) often compare the binding energies with an upper limit to decide whether the species should be desorbed. However, binding energies are relatively uncertain and astrochemical results can be very sensitive to changes in their adopted values (Wakelam et al., 2017).

Grain Surface Reaction

Three mechanisms have been proposed for the reactions happening between two species on a grain surface, including the Langmuir-Hinshelwood, the Eley-

Rideal, and the "hot atom" mechanism (Herbst & Van Dishoeck, 2009; Cuppen et al., 2017). The Langmuir-Hinshelwood, or so-called diffuse mechanism, is for reactions happening between two ice-phase species. In contrast, the Eley-Rideal mechanism has the approach of stick-and-hit, where one ice-phase species is hit by a gas-phase species. "Hot-atom" is an in-between mechanism, where a non-thermalized species travels on the surface until reacting with another species. The Langmuir-Hinshelwood is the most widely used. To derive its formula, it assumes the reactants are absorbed by dust and diffuse on the grain surface by tunnelling or thermal hopping over barriers between sites until they meet each other. The reaction rate is estimated by:

$$k_{LH} = \kappa_{ij}(k_{scan,i} + k_{scan,j}), \tag{3.12}$$

where $\kappa_{ij} = e^{-E_a/kT_d}$ is the occurrence probability of the reaction with an activation barrier E_a and $k_{scan} = k_{hop}/N_s\sigma_d$ is the scanning rate. $N_s\sigma_d$ is the number of binding sites per grain and k_{hop} is the hopping rates expressed by:

$$k_{hop} = \nu_0 e^{-E_{diff}/kT_d}, \tag{3.13}$$

where E_{diff} is usually estimated by multiplying a factor to the binding energy fE_b. In this case, tunnelling is faster than the hopping rate. κ_{ij} is replaced by:

$$\kappa_{ij} = e^{\frac{-2a}{\hbar}\sqrt{2\mu E_a}} \tag{3.14}$$

and k_{hop} is replaced by:

$$k_{hop} = \nu_0 e^{\frac{-2a}{\hbar}\sqrt{2\mu E_{diff}}}. \tag{3.15}$$

In addition to the reactions between two ice-phase species, the larger molecules on the grain surface may also be dissociated by UV photons (Walsh et al., 2014), including the secondary photons. The reaction rates are assumed to be the same as the equivalent gas-phase reactions, i.e.:

$$k = \alpha e^{-\gamma A_V} \tag{3.16}$$

and have the same self-shielding effects.

3.4 Chemical Model Examples

In this section, we briefly introduce the chemical networks used in this thesis.

Protoplanetary Disk Chemical Network

Based on the UMIST database published in 2006 (Woodall et al., 2007), Walsh et al. (2010) built a chemical network by extending the gas-phase reactions with gas-grain interactions and grain-surface reactions and implemented the model in private Fortran codes. The code was then updated several times in several papers (Walsh et al., 2012; Walsh et al., 2013; Walsh et al., 2014; Walsh et al., 2015). In the version used in this work, the gas-grain interactions include freeze-out (Hasegawa et al., 1992), thermal desorption (Hasegawa et al., 1992), photodesorption (Willacy, 2007) and cosmic-ray-induced desorption (Hasegawa & Herbst, 1993). The grain surface reactions include the photon-dissociation of grain surface species (Walsh et al., 2014) and surface reactions proceeding through the Langmuir-Hinshelwood mechanism. The reactive desorption (Garrod et al., 2007) induced by the grain surface reactions is also included.

UCLCHEM Network (v1.3)

`UCLCHEM` is a time-dependent gas-grain chemical code written in Fortran (Viti, 2013; Holdship et al., 2017). The code was published with a network extended from the UMIST database, but it also supports the generation of reduced networks from the full network by limiting the reactants and products. The whole chemical network contains the gas-phase reactions from UMIST and gas-grain interactions, including freeze-out, thermal desorption, photodesorption, cosmic-ray-induced desorption and H_2 formation desorption. The rates of these reactions are based on the model proposed in Rawlings et al. (1992, freeze-out), Collings et al. (2004, thermal desorption) and Roberts et al. (2007, photodesorption, cosmic-ray-induced desorption and H_2 formation desorption). For surface reactions, it builds a simple model by merging hydrogenation with freeze-out and leaving freedom for users to decide the branching ratios. For example, when CO sticks on grain mantles, it could be hydrogenated and form CH_3OH and users are allowed to set in a pre-defined grain file that, for example, 90% of CO becomes grain-phase CO and the remain-

ing 10% becomes CH_3OH. The whole package also includes hydrodynamics sub-grid models, like C-shocks and evolving conditions of molecular clouds. However, these sub-grid models do not involve solution of the Euler equations and the hydrodynamics modules are single zone or multiple one-zone models.

In our studies, we adopted a reduced network extracted from `UCLCHEM` by limiting species. The reduced network was benchmarked with the model from Walsh et al. (2015). To make the models have a good agreement, we modified the model used in `UCLCHEM` to make it use the thermal desorption rate from Hasegawa et al. (1992) and photon-desorption rate from Willacy (2007) as in Walsh et al. (2015). We also changed the binding energies of species, based on those used in the study of Entekhabi et al. (2022).

Deuterium Fractionation Network

In the local ISM, the D/H ratio has been estimated to be around 1.6×10^{-5} (Linsky, 2007). Deuterium atoms are formed during big bang nucleosynthesis and then partially destroyed by nuclear fusion in stars as well as recycled from this processed gas back into space via stellar winds, supernovae, etc. However, on Earth, in comets or in some observed prestellar cores, the D/H ratios of certain molecules are much higher than the local average D/H value. For example, the ratio of N_2D^+ to N_2H^+, which are recognized as good tracers of prestellar cores, has been observed to reach $\gtrsim 0.1$ (Crapsi et al., 2005; Pagani et al., 2007; Miettinen et al., 2012; Kong et al., 2016). These pieces of evidence support the occurrence of deuterium fractionation. Theories also support the occurrence of deuterium fractionation inside prestellar cores. The D/H ratio in the subsequent protoplanetary disk, planetesimals/comets and planets then can be explained by the inheritance of species left from the prestellar core phase. However, the details of the process by which this may occur are still under debate.

Theoretically, the deuterium fractionation process can be approximately divided into three steps (see Figure 3.2). First is the formation of H_3^+, which occurs via the reactions:

$$\begin{aligned} H_2 + CR &\rightarrow H_2^+ + e^- + CR \\ H_2^+ + H_2 &\rightarrow H_3^+ + H. \end{aligned} \tag{3.17}$$

Being charged, H_3^+ is more reactive than neutral species. The H_3^+ then reacts

with HD, which is the main reservoir of D atoms, and forms H_2D^+:

$$H_3^+ + HD \rightarrow H_2D^+ + H_2. \tag{3.18}$$

The inverse reaction could also occur, i.e., destroying H_2D^+ and forming HD. However, there is a small activation barrier for this inverse reaction. If the temperature is low enough, the environment has a tendency to form H_2D^+, which is the beginning of the deuterium fractionation process. H_2D^+ then could continue to react with HD to form D_2H^+ and D_3^+.

$$\begin{aligned} H_2D^+ + HD &\rightarrow D_2H^+ + H_2 \\ D_2H^+ + HD &\rightarrow D_3^+ + H_2 \end{aligned} \tag{3.19}$$

The formed H_2D^+, D_2H^+ and D_3^+ may then react with other gas-phase species leading to formation of deuterated molecules and molecular ions. Or they may undergo dissociative recombination with electrons to form gas phase D atoms, which may then undergo grain surface reactions to form deuterated ice species.

Since H_2D^+ plays a central role in the transfer of D into species and since its abundance increases in cold gas, deuterium fractionation is expected to be enhanced generally in such cold conditions. Furthermore, as the formation of H_2D^+ relies on H_3^+ as a precursor, it means that a higher cosmic ray ionization rate also accelerates the deuteration process. In addition, as H_3^+ is destroyed by O and CO, removing these species from the gas phase, e.g., by freeze-out onto dust grain ice mantles, also enhances deuterium fractionation. Thus, cold and dense regions of prestellar cores and clumps are ideal places for enhanced deuterium fractionation.

Another important factor influencing deuterium fractionation is the ortho-and-para ratio of molecular hydrogen (OPR^{H_2}). The internal energy of ortho-H_2 in its ground state is enough to overcome the endothermic energy barrier in the inverse reaction of Equation 3.18 (i.e., $H_2D^+ + H_2 \rightarrow H_3^+ + HD$). As a consequence, the ratio of H_2D^+/H_3^+ is suppressed and limits the third step of deuteration. Theoretically, H_2 formed on dust grains is expected to have a 75% probability to form ortho-H_2 and 25% probability to form para-H_2.

Subsequently, the ratio decreases over time via reactions with H^+ and H_3^+ (e.g.: H^++o-$H_2 \rightarrow H^+$+p-H_2; p-H_3^++o-$H_2 \rightarrow$ o-H_3^++p-H_2) (Hugo et al., 2009; Honvault et al., 2011), especially in cold and dense gas. Due to the low temperature ($\sim$ 20 K), the OPR^{H_2} is predicted to be low ($\sim$ 0.001) in star-

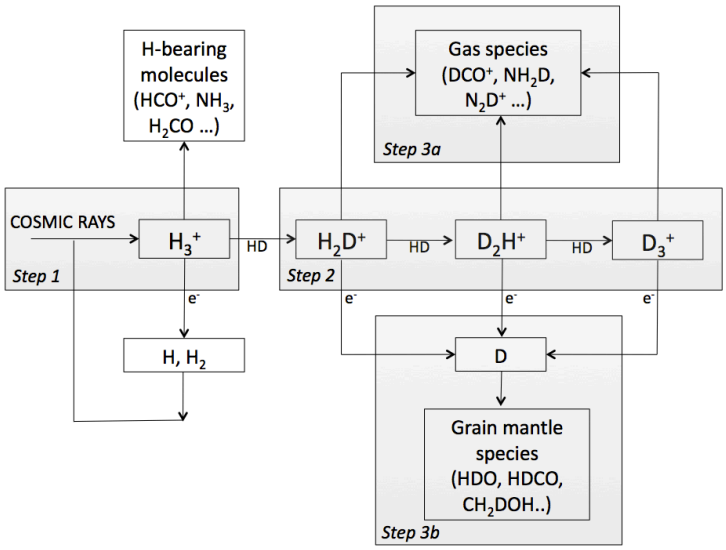

Figure 3.2: Schematic overview of the processes leading to deuterium fractionation (Credit: Ceccarelli et al., 2014).

forming environments (e.g., Sipilä et al., 2013; Brünken et al., 2014).

A variety of astrochemical studies have been carried out to model deuterium fractionation. Walmsley et al. (2004) considered a reduced chemical network, including the nuclear spin states of H_2, H_2^+, H_3^+ and H_2D^+. This network assumed heavy elements, like C, N, O, etc., are fully depleted. Extending this work, Flower et al. (2006), Hugo et al. (2009), Pagani et al. (2009) and Sipilä et al. (2010) included updated reaction rates for spin states and deuterated forms of H_2 and H_3^+. Vastel et al. (2012) presented networks including molecular species with up to three atoms. Kong et al. (2015) extended these works to include H_3O^+ to acquire more precise results. As a consequence, the abundances of electrons, water, HCO^+, DCO^+, N_2H^+, N_2D^+ are improved and have a good agreement with the even more extensive network of Sipilä et al. (2013). More recently, Majumdar et al. (2017), based on the work of Wakelam et al. (2015), presented a complete network including spin state chemistry with 13 elements (H, He, C, N, O, F, Na, Mg, Si, P, Cl, S, Fe). Sipilä et al. (2019) further studied the influence of different treatments of ion-molecule proton-donation reactions. In our work, we have adopted the network from Kong et al. (2015), together with modest improvements suggested by the results of Majumdar et al. (2017).

CHAPTER 4

Chemodynamics

In Chapter 3, we have described the complexities and limitations of astrochemical models, which is derived, in part, from the variety of different methods of implementing reactions and the many associated uncertainties, e.g., in values of binding energies, photon yields, etc. Nevertheless, it is a long term goal for the astrochemistry research community to improve these models so that they can be used to more accurately interpret conditions and proceses in the ISM. However, one major limitation of these models is that they are often implemented in a simple single zone, i.e., zero-dimensional, framework. Such an implementation ignores the influence of dynamical effects, especially more complex evolutionary histories of physical quantities, such as density and temperature, and abundance changes due to advection. To further understand the influence of such effects, three-dimensional chemodynamical simulations are needed. Previous work on such simulations, of varying levels of complexity, has been presented by several groups (see, e.g., Glover et al., 2010; Hincelin et al., 2016; Körtgen et al., 2017; Bovino et al., 2019; Smith et al., 2020).

4.1 Magnetohydrodynamics to Chemodynamics

A typical ideal magnetohydrodynamics (MHD) simulation solves the following equations:

$$\frac{\partial \rho}{\partial t} + \boldsymbol{\nabla} \cdot (\rho \mathbf{v}) = 0, \tag{4.1}$$

$$\frac{\partial \rho \mathbf{v}}{\partial t} + \boldsymbol{\nabla} \cdot (\rho \mathbf{v}\mathbf{v} + \mathbf{I}P - \mathbf{B}\mathbf{B}) = -\rho \boldsymbol{\nabla} \phi, \tag{4.2}$$

$$\frac{\partial E}{\partial t} + \boldsymbol{\nabla} \cdot [(E + P)\mathbf{v} - \mathbf{B}(\mathbf{B} \cdot \mathbf{v})] = -\rho \mathbf{v} \cdot \boldsymbol{\nabla} \phi - \Lambda + \Gamma, \tag{4.3}$$

$$\frac{\partial \mathbf{B}}{\partial t} - \boldsymbol{\nabla} \times (\mathbf{v} \times \mathbf{B}) = 0, \tag{4.4}$$

where $\rho, \mathbf{v}, P, E, \mathbf{B}, \phi$ are the density, velocity vector, pressure, energy density, magnetic field vector and gravitational potential, respectively. Here, $\mathbf{I}$ is an identity tensor, while Λ and Γ represent the cooling and heating rates, respectively. To include the contributions of magnetic fields, the pressure and energy are given by:

$$P = p + \frac{B^2}{2}, \tag{4.5}$$

$$E = e + \frac{\rho v^2}{2} + \frac{B^2}{2}, \tag{4.6}$$

where p and e are thermal pressure and thermal energy density, respectively. The magnetic permeability (μ_0) is unity in these equations. In the case of ideal gas with a ratio of specific heats γ, the thermal energy can be expressed as:

$$e = \frac{p}{(\gamma - 1)}. \tag{4.7}$$

If the ideal gas is isothermal, the thermal energy can also be expressed in terms of the sound speed (c_s):

$$c_s = \sqrt{\frac{\gamma k T}{\mu m_H}}, \tag{4.8}$$

i.e., in the form:

$$e = \frac{\rho c_s^2}{\gamma(\gamma-1)}. \tag{4.9}$$

Equations 4.1 to 4.3 represent the conservation of mass, momentum, and energy, while Equation 4.4 is the magnetic induction equation. To extend a fluid to a reactive flow, the equation of species abundance evolution must also be included:

$$\frac{\partial n_i}{\partial t} + \boldsymbol{\nabla} \cdot (n_i \mathbf{v}) - \boldsymbol{\nabla} \cdot (\mathcal{D} \boldsymbol{\nabla} n_i) = C(n_i, n_j, T) - D(n_j, T) n_i, \tag{4.10}$$

where n_i represents the number density of each species and the summation of number density weighted by mass must equal to mass density ($\sum_i n_i m_i = \rho$). This equation includes three processes: advection, diffusion and chemical reactions. The second and the third terms on the left-hand side represent the advection and the molecular diffusion processes, respectively. The right-hand side terms refer to the construction (C) and destruction (D) of ith species. In astrophysical flows, the molecular diffusion term is usually ignored, given its slow expected rate. Turbulence also induces advective diffusion, but the effect is difficult to include accurately, especially given the difficulty of resolving the scales associated with a turbulent cascade.

Equation 4.10 can be split into two parts:

$$\frac{\partial n_i}{\partial t} + \boldsymbol{\nabla} \cdot (n_i \mathbf{v}) = 0 \tag{4.11}$$

$$\frac{dn_i}{dt} = C(n_i, n_j, T) - D(n_j, T) n_i. \tag{4.12}$$

The first equation only considers the advection term and the second equation solves the reactions, which is the same set of differential equations handled by one-zone astrochemical models (See Chapter 3). That is to say, to implement a chemodynamical simulation, we need to make the hydrodynamics code calculate the advection and then insert the astrochemical model to solve the reactions.

4.2 Simulation Codes

The implementation of a chemodynamical simulation is usually done by adding passive scalar fields into hydrodynamics code. The hydrodynamics codes can be either mesh (Euler method) or meshless (Lagrangian method) codes (e.g. Grassi et al., 2017; Bovino et al., 2019). The latter gives an advantage of zero advection error of elemental conservation. Besides passive scalar fields, a different approach is inserting tracer particles into simulations and evolving chemistry according to the time-dependent densities and temperatures. This post-processing approach traces the chemical evolution, but loses the effect of advection (e.g., Hincelin et al., 2013; Hincelin et al., 2016). In this section, we introduce the codes and implementations used in this thesis. These all involve implementing passive scalar fields in mesh code `Enzo`.

Enzo

`Enzo`(Bryan et al., 2014; Brummel-Smith et al., 2019) is an adaptive mesh refinement (AMR) hydrodynamics code, developed originally for cosmological simulations. It has a good connection with the `GRACKLE` (Smith et al., 2017) chemistry library to calculate the evolution of primordial gas. `GRACKLE` also supports the calculation of heating/cooling rates of primordial gas and metals and some UV background radiation effects. However, the main purpose of `GRACKLE` is primordial chemistry. Although it can be extended to include some user-defined `Cloudy` heating/cooling tables, it is not practical to make it include a general chemical network of the ISM.

KROME

`KROME` is a chemistry package working as a Python-based parser to convert a user-provided chemical network to Fortran codes. Users have the freedom to define their own reaction format by using its pre-defined tokens. It provides a unique interface function so that it can work with other hydrodynamics codes. However, it does not guarantee consistency with hydrodynamics codes. Users have to ensure that all species in the network exist in the hydrodynamics codes and that the advection is handled by the hydrodynamics codes (see Section 4.1). Besides, because it generates source codes, these codes have to be compiled with the hydrodynamics codes to make the whole combina-

tion work. It also provides some official patches for several hydrodynamics codes, including `FLASH`, `Enzo`, `GIZMO` and `RAMSES`. For `Enzo`, the patch does not handle advection and the existence of species. Users have to define the additional species and modify some routines for advection and renormalization (e.g., `Grid_SolveHydroEquations.C` for PPM, Zeus, MHD_Li/CT solvers and `Grid_UpdatePrim.C` for Runge-Kutta solvers).

Naunet

Inspired by `KROME`, we have developed a python package, `Naunet`, to convert any chemical network into C++ codes. Instead of the approach of `KROME`, in which users have to manually convert any existing network into its compatible format, we implemented multiple interfaces to read reactions in different formats from different sources. We also implemented built-in grain models so that users can easily select the model they would like to apply in their network. This feature is particularly useful for benchmarking tests. The usage of our package is supported both in a python module and in a command line tool. Users can construct their networks in python scripts by adding reactions one by one or they can simply use the command line tools to deal with the input text files. The former way can provide more freedom to customize the network and both ways can effectively generate the C++ codes. The generated codes can be further wrapped into C++ static libraries, shared libraries and python modules so that users can do the chemical modeling in C++ or in python. The highly modularized design allows users to switch between models quickly.

Another advantage of `Naunet` is the multiple solvers it supports. Currently, we have implemented four kinds of solvers from `Sundials` package (Hindmarsh et al., 2005; Gardner et al., 2022) and `Boost` library. Users can test the performance of different solvers and choose the one with the best performance for their work. In general, the KLU solver, which solves the ODE systems via sparse matrices, from the `Sundials` package has a better performance. In the next section, we will show various performance test results.

4.3 Performance

A problem of chemodynamical simulations is the memory usage from the number of species. To track the evolution and calculate the advection of passive scalar fields, the density of each species must be stored in each grid. As the number of species increases, the simulation also occupies more disk storage and memory. For example, a magnetohydrodynamical simulation usually stores about 10 fields (typically, $\rho, \mathbf{v}, E, \mathbf{B}$ and some optional fields like internal energy or gravitational potential). However, an ISM chemical network may contain hundreds of species. For example, if the network contains about 100 species, the simulation with the resolution of 128^3 will use about 2GB of memory. If the resolution is enhanced to 512^2, the simulation data will exceed 100GB. The number of species limits the resolution and increases the loading of communication when the simulation is running on many CPUs in a cluster.

A simple way to save memory and disk storage is using the AMR structure to limit the finer grids focusing on subregions in the simulation. The way is effective if the interesting regions are only a small portion of the whole domain. However, the finest resolution is surely less than the same ones without chemistry. The refinement also derives a side effect from the interpolation error. Although most of the popular AMR codes support high-order interpolation methods and conservative interpolation to reduce numerical errors, element abundance conservation can still be broken (Grassi et al., 2017). The problem is that gradient limiters and interpolation weights can be different for each species. Even if each individual chemical species is conserved during the interpolation, the summation of atoms in species may not be conserved. This means the number of species should be normalized twice after advection: once for element conservation (including charge) and once for mass conservation.

Besides memory, the most significant universal problem of chemodynamical simulations is their bad performance when implementing large networks. Since a larger network means more species and more reactions, it means that more equations and a larger matrix need to be solved. The cost of computational resources is significant as the network size grows. Generally, an ISM chemical network contains thousands of reactions and hundreds of species. Even if it may only take a few milliseconds to finish one step in one grid cell, the cost becomes significant when there are 10^6 (the order of 128^3 resolution) grids. Figure 4.1 shows the mean time of one step of chemodynamical simulations in a 64^3 domain. The simulations use the same initial condition but were coupled

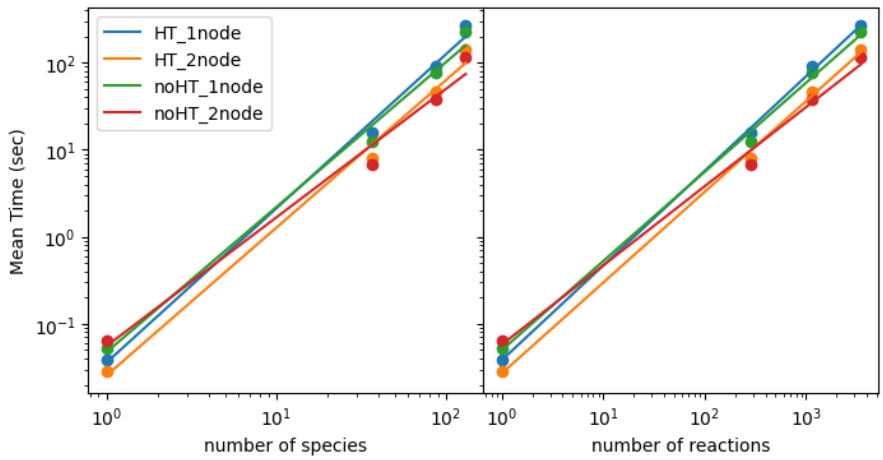

Figure 4.1: Computational time of chemodynamical simulations with different sizes of chemical networks. The left panel shows the mean time versus the number of species and the right panel shows the mean time versus the number of reactions. The same simulation is run with different architectures (HT- with hyper-threading, noHT - without hyper-threading) and different processors (1node - 64 cores, 2node - 128 cores). The test is done on Vera cluster of Chalmers University of Technology in Gothenburg, Sweden (C3SE). The nodes are built with Intel Xeon Gold 6130 CPUs and have 92GB of memory on each node.

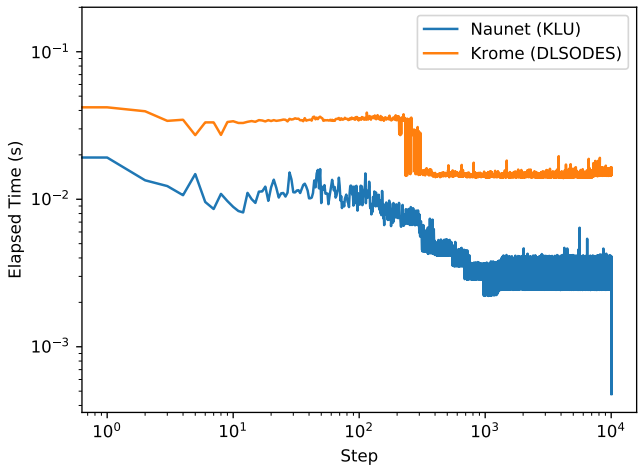

Figure 4.2: The elapsed time in each step of `Naunet` (blue) and `KROME` (orange). The test is done by the single grid model of the deuterium fractionation network (see Section 3.4) on Intel Xeon Gold 5118 CPU.

with different sizes of networks by `KROME`. We see that the computational time is almost directly proportional to the number of reactions and roughly has a power of 1.7 with the number of species. Note that the performance could also be influenced by the initial conditions. For example, if the temperature of some grids is out of the valid range of reactions, the reaction rates are zeros and could make the calculation faster. However, in general, the performance of simulations can be a thousand times slower than a simulation without chemistry, if a network containing thousands of reactions is used. For example, we need to wait over forty days for a simulation originally taking one hour, which can become impractical.

This long-known issue of computational performance leads to a demand for higher-performance ODE solvers. Several algorithms have been proposed to efficiently solve ODE systems. In the aspect of astrochemistry, Nejad (2005) compared the performance of several stiff ODE solvers from `ODEPACK` and `GEAR` packages. It was found that the LSODES solver, which is also the solver used in `KROME`, generally has a better performance for its capability of

taking advantage of sparse matrices. Furthermore, it was also found that the performance of chemical modeling can be improved by resorting the order of the species to make a bottom-heavy Jacobian matrix. However, the legacy solvers like LSODES lack the capability of vectorizing, which is a common feature supported by modern CPUs. The KLU solver adopted in `Naunet` supports both the sparse matrix and vectorizing and is usually faster than the LSODES solver by a factor of three (see Figure 4.2). Apart from the algorithm, several methods can improve the performance of chemodynamical simulations:

- Parallelization: Parallelization is a common way to improve the performance of simulations. Currently, `openmp` and `MPI` have been widely applied in numerical codes. `Enzo` also supports the usage of `MPI`, which can accelerate the simulation by requesting more processors from more nodes in a cluster. Figure 4.1 also shows the simulation is almost two times faster by using two nodes rather than one node. However, it is also impractical to offload the heavy computation by requesting hundreds of nodes. Graphics cards could be another choice of parallelization. By using the graphics processing units (GPU) on graphics cards, hydrodynamics simulations could be ten times faster than on a CPU (e.g., Schive et al., 2018). Note this also depends on the frequency and the number of units. Usually, these kinds of tests are done under the same "cost" of a specific cluster. Several studies are working on moving the differential equation solvers onto GPU (Zhou et al., 2011; Niemeyer & Sung, 2014; Ahnert et al., 2014; Curtis et al., 2016; Stone et al., 2018). However, these studies are focusing on combustion engineering and biochemistry. They have not been ported to astrochemistry and have several drawbacks. Most solvers are explicit and cannot handle the level of stiffness in astrochemical networks. Some of these solvers use the first-order implicit backward differential formula (BDF) method and lose accuracy, while other higher-order solvers often have performance problems, e.g., because of their instability and more complex timestep assignments. Astrochemical networks are generally expressed as sparse matrices and if ODE solvers can take advantage of this sparseness, then performance is improved (Grassi et al., 2014). However, most of the GPU-ported solvers assume the matrices are dense and do not take advantage of this feature. Recently, Balos et al. (2021) introduced a GPU-based stiff

ODE solver in `Sundials` and this may be a promising way to offload the computation onto GPUs.

- Reducing the size of network: As the computational load is highly related to the size of the network, it is intuitive to reduce the load by reducing its size. This idea has been studied for a long time. A typical way is done by pre-selecting species and related reactions (Nelson & Langer, 1999). Our `UCLCHEM` reduced network is also derived by selecting species. This approach is useful when estimating the most abundant species. The small abundances of rarer heavy elements hardly change the abundances of simple C-bearing or O-bearing molecules. However, it obviously cannot predict the abundances of species involving these heavy elements since they were not selected. Another approach assumes that some species stay with equilibrium abundances to focus on solving the non-equilibrium species (Lam, 1993; Glover et al., 2010), where those equilibrium species are chosen by those with rapid reaction rates. However, this approach may not be valid for a wide range of parameters because of the variation of reaction rates. A further scheme is then to try to dynamically reduce the reactions to avoid this limitation (Tupper, 2002; Grassi et al., 2012).

- Reducing the number of chemical time steps: This could be the simplest way to accelerate the simulations, but the method only works when the chemical timescale is much longer than the hydrodynamics timestep. If the hydrodynamics timestep is much shorter than the chemistry timescale, the chemistry calculation can be operated only every several hydrodynamics timesteps and thus keep a relatively good approximation for the abundances. This approach has been implemented in this work. However, if the simulation is undergoing fast heating/cooling, this approach will lose accuracy.

- Neural network: Due to the advance of deep learning methods, neural networks have become a popular tool in a variety of fields. As the fundamental neural network, artificial neural networks also have been widely applied in computational chemistry, biochemistry, etc. (Goncalves et al., 2013). A recent work also applies the method to create an emulator of `UCLCHEM` (De Mijolla et al., 2019). Similarly, Branca & Pallottini (2022) probed the potential of using Physics Informed Neural Networks (PINN)

to reproduce ISM chemical evolution. However, they only tested a small network composed of 46 reactions and it already needs 10^3 GPU hours to train a model. In the context of replacing ODE solvers, Chen et al. (2018) proposed the `neuralODE` model and investigated the possibility to use it to mimic general ODE solvers. Although chemical emulators can skip the cost of solving differential equations and reproduce, approximately, the nonlinear results, a general problem of these black boxes is how to train a valid model and guarantee the correctness over a wide range of parameter space and whether there is a general way to train an effective model.

CHAPTER 5

Summary of included papers

5.1 Paper I

In this paper, we focus on deuterium fractionation in massive prestellar cores (Figure 5.1). The reason is that N_2H^+ and its deuterated form N_2D^+ have been observed in several prestellar cores and are thought to be good diagnostic tracers of these objects (Caselli et al., 2002; Tan et al., 2013; Kong et al., 2016). From a theoretical point of view, cold and dense gas is also an ideal place for deuterium fractionation (see Section 3.4). The emission lines of these species may also be useful to interpret the kinematics in the cores. Following the study of Goodson et al. (2016), we also use the gas phase chemical network of (Kong et al., 2015), but with minor updates from (Majumdar et al., 2017). The network contains species composed by heavy elements, C, N, and O, and we investigate the influence of parameterized depletion factors of these species. We then use `Enzo` and `KROME` to couple the chemical network with a magnetohydrodynamics simulation of a massive prestellar core.

The work presented focuses on the influence of chemical parameters on the abundances of species within a particular prestellar core. Its initial conditions are set to a mass of 60 $M_\odot$ and a mass surface density of the background

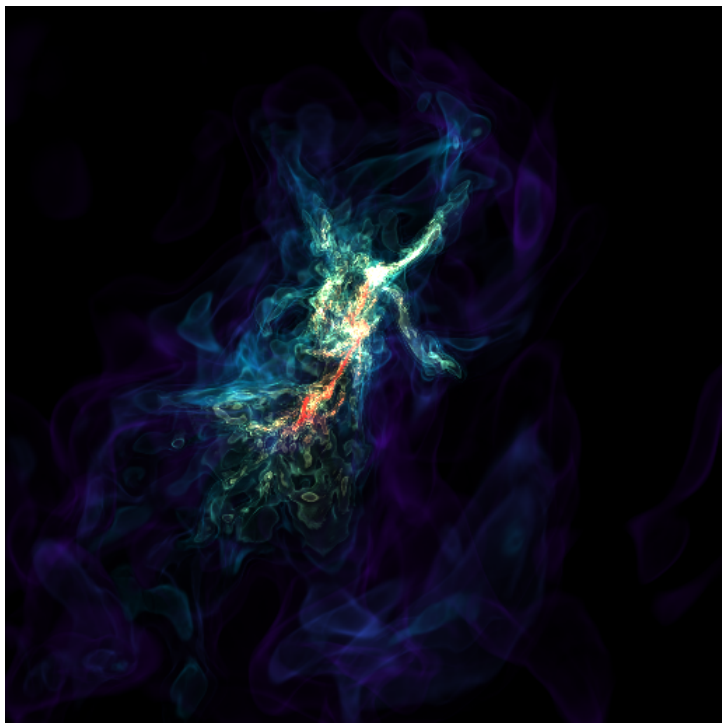

Figure 5.1: A collapsing massive prestellar core.

clump environment of 0.3 g cm^{-2}. Within the context of the Turbulent Core Accretion (TCA) model, these conditions then imply that the core has a radius of 0.1 pc. The mean density of the core is thus set to be $n_{\rm H} \simeq 4\times10^5\,{\rm cm}^{-3}$ and its freefall time is 76 kyr. The core is assumed to be approximately isothermal at a temperature of 15 K. It is initialized with a turbulent velocity field and a cylindrically symmetric magnetic field to make the core slightly supervirial in the beginning. Since there is no driving of the turbulent velocity field, the core will begin to collapse as turbulence decays. The chemical parameters we study are the initial OPR^{H_2}, temperature, cosmic ray ionization rate and depletion factor of CO and N (two factors, one controlling the abundances of C and O, another one controlling the abundance of N) and the initial chemical age, i.e., affecting initial abundances. We follow the chemical evolution in the core for 0.8 free-fall times and analyze the number densities and column densities of N_2H^+ and N_2D^+.

Figure 5.2 shows the comparison of abundances with observational data. We conclude that one model with high cosmic ray ionization rate (1.0×10^{-16} s^{-1}) and high depletion factor ($f_D^{\rm CO} = 1000$, $f_D^{\rm N} = 100$) is one of the best models for matching observational data of massive PSCs. The abundances also allow us to estimate the velocity gradient, the velocity dispersion, the rotational energy, the kinetic energy and the virial parameter of the simulated core as would be traced under the assumption of optical thin emission of N_2D^+(3-2). Overall, the rotational energy is small compared with the gravitational energy. The core can appear subvirial in certain directions during much of the evolution because of the contribution of magnetic fields to its support.

Although we found one possible way for the prestellar core to reach a high deuterium fraction, comparable with some observed systems, the fast collapse rate may also influence the results. For example, if the prestellar core had stronger $B-$field support and collapsed more slowly, then a lower cosmic ray ionization rate would likely be allowed to enable a similar level of deuteration to be reached. One way to potentially distinguish between these scenarios of fast and slow collapse is to examine the properties of the core kinematics as traced by N_2H^+ and N_2D^+.

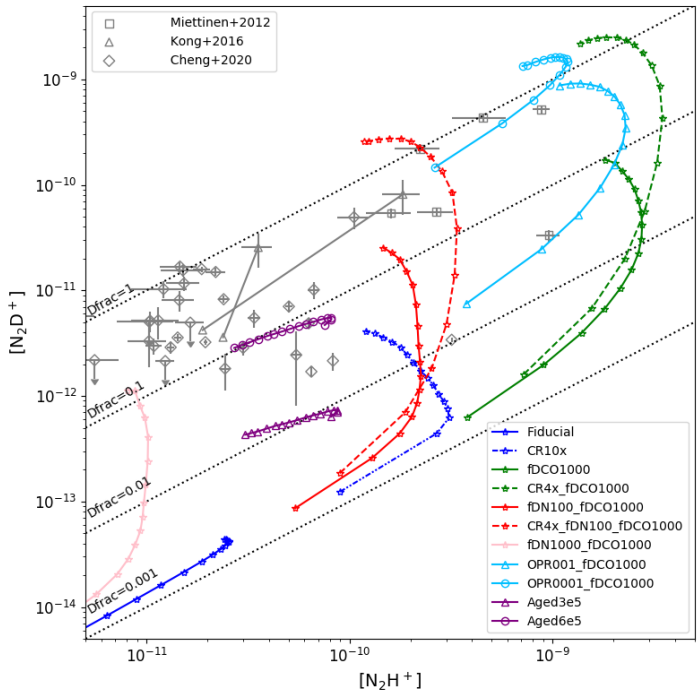

Figure 5.2: Time evolution of the average abundances of N_2H^+ and N_2D^+ in massive PSC simulations, as listed in the lower right legend. The grey squares, triangles and diamonds are observational data from Miettinen et al. (2012), Kong et al. (2016), and Cheng et al. (2021).

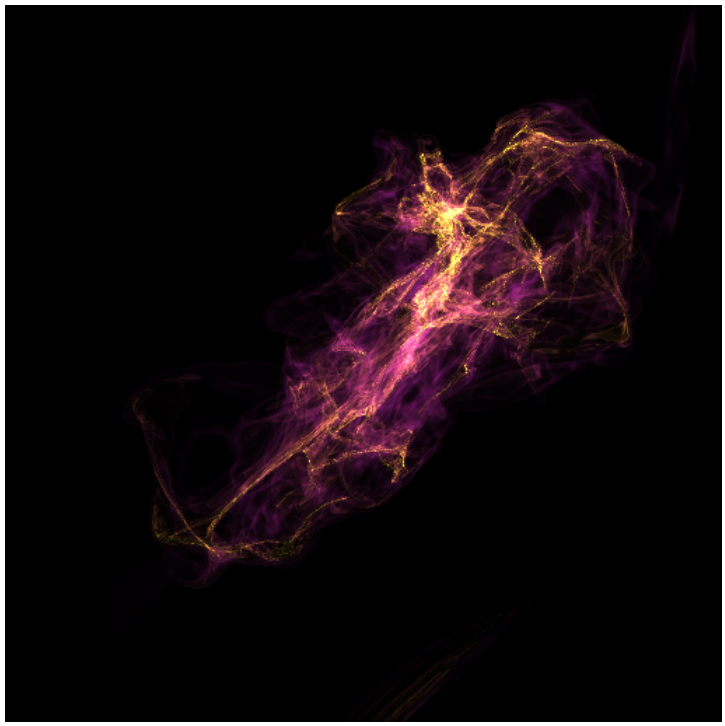

Figure 5.3: Filamentary structure derived from two merging clouds in a weak magnetic field (10 μG).

5.2 Paper II

In this paper, we extended the previous work on simulating the collision of two giant molecular clouds (Wu et al., 2017). The goal is to understand whether clumps/protoclusters forming from colliding clouds or non-colliding clouds show any differences in their CMFs. While the focus of this paper is purely on the physical properties of the system, this is important preparatory work for the chemodynamical study of Paper III.

We followed the same settings to simulate colliding and non-colliding magnetized GMCs with the highest resolution in the series of papers (Figure 5.3). The resolution is up to 0.015625 pc, i.e., 3,200 au, and enables us to resolve the prestellar cores in the simulation. With the cores identified by dendro-

gram (Rosolowsky et al., 2008) on mass surface density maps, we studied the evolution of core mass functions derived from each case. To further compare with observations, we also applied CASA (McMullin et al., 2007) to create synthetic ALMA observation. We examine the power-law of the CMFs derived from simulations and synthetic ALMA observation in multiple ranges ($M > 10\ M_\odot$, $1\ M_\odot < M < 10\ M_\odot$, and $M > 1\ M_\odot$). In the colliding case, we found that the high-mass end of the CMFs can be fit by a power law $dN/d\log M \propto M^{-\alpha}$ with $\alpha \simeq 0.6 - 0.7$, i.e., relatively top-heavy compared to a Salpeter mass function. The non-colliding GMCs form fewer cores with a CMF with $\alpha \simeq 0.8$ to 1.2, i.e., closer to the Salpeter index. The synthetic ALMA observation has an effect of smoothing CMFs and making them closer to a single power-law function. Without the ALMA-filtering effect, the CMFs usually show flat curves in the range of $1\ M_\odot < M < 10\ M_\odot$. These results are compared with observational data from Cheng et al. (2018) and Liu et al. (2018) and O'Neill et al. (2021). The CMFs from the colliding case and the three datasets are shown in Figure 5.4.

We also examine the core properties, including mass, size, density, velocity, velocity dispersion, temperature and magnetic field strength. We found that cores formed from colliding clouds are typically warmer, have more disturbed internal kinematics and are more likely to be gravitationally unbound, than cores formed from non-colliding GMCs.

5.3 Paper III

Here we study the evolution of chemical species within the framework the GMC simulations (Figure 5.5), both colliding and non-colliding, presented in Paper II. In Wu et al. (2017) and Bisbas et al. (2017), PDR models were applied to postprocess outputs of these types of simulations to predict emission from CO molecules, including high J line emission, and from CI, CII and OII. The aim is to understand the signatures from the collisions of GMCs. However, such postprocessing does not accurately follow the history of chemical evolution.

To obtain a more accurate and general understanding of the chemical abundances, we couple a reduced chemical network extracted from `UCLCHEM` (see Section 3.4) with the simulations. We simulate the colliding and non-colliding clouds in the weak magnetic field case and study chemical evolution under dif-

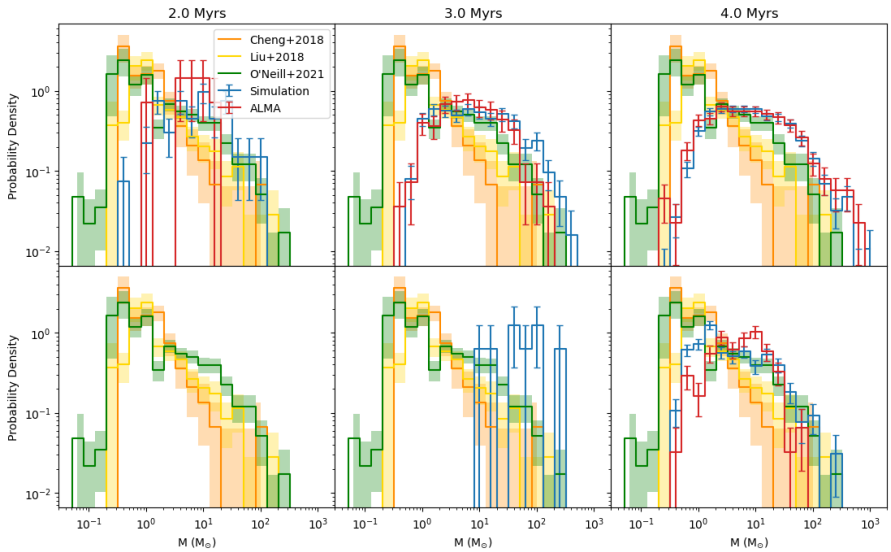

Figure 5.4: The probability distribution function (PDF) of core mass functions (CMFs) at 2 Myr (left column), 3 Myr (middle column) and 4 Myr (right column) for the colliding case. The blue lines show original simulation results and the red lines show those after ALMA filtering. The error bars indicate the Poisson counting errors. The top set of six panels show comparison to observational "raw" CMFs from Cheng et al. (2018) and Liu et al. (2018) and O'Neill et al. (2021). The bottom set of six panels show the observational "true" CMFs, i.e., after flux and number correction, from these studies.

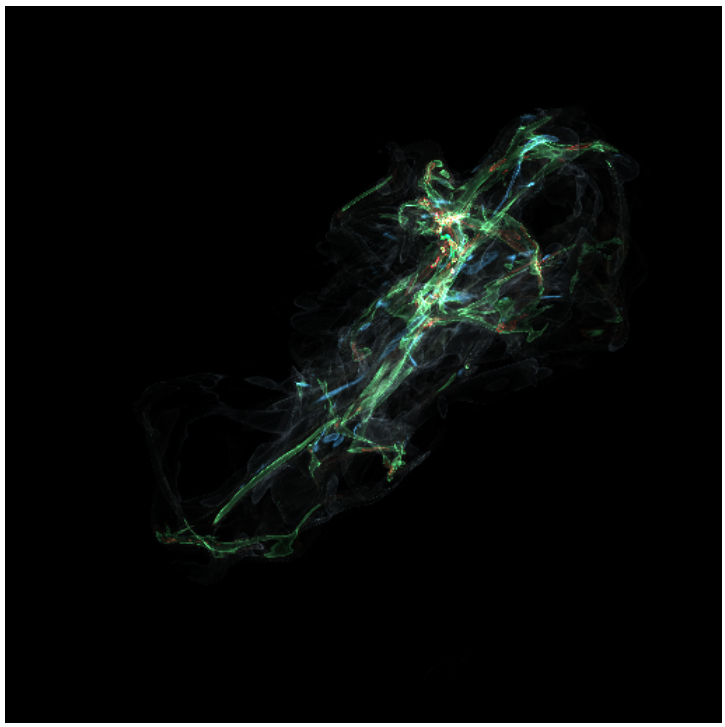

Figure 5.5: Cloud-cloud collision derived filamentary structure viewed in C (blue), CO (green), and ice-phase methanol (red).

ferent cosmic ray ionization rates. We first examine the chemical abundances, particularly C and O reservoirs on large scales. The results show the transition of elemental C from C^+ to C and then CO, while the excess O that is not in CO transitions from O to water ice. We then examine the abundances of gas tracers, especially CO, HCO^+ and N_2H^+ of high density regions selected in the GMCs. These results are compared with observations of IRDC clumps to derive constraints on chemodynamical history and cosmic ray ionization rate. As part of this study, we also compare our results to those derived using more approximate, single zone models.

5.4 Summary of other papers and projects with major contributions

Several other papers and projects have also been associated with the research developed in this thesis. The study of Entekhabi et al. (2022) included a large parameter study of a gas-grain chemical network, i.e., over density, temperature, visual extinction, cosmic ray ionization rate and time. The effects of different efficiencies of cosmic-ray-induced thermal desorption and different values of CO ice binding energy were also investigated. Two main grids of models were run and their results were used to benchmark our developed reduced chemical network based on UCLCHEM that was implemented in Paper III. In addition, the study of Entekhabi et al. (2022) used IRAM-30m telescope observations to derive abundances in ten dense clumps in the massive IRDC G28.37+0.07. These data were then used for comparison to our chemodynamical simulation results of Paper III.

The study of Cevallos Soto et al. (2022) implemented the same gas-grain network in a 1-D (radial) model of protoplanetary disk midplanes. The main innovation was to include advective transport of radially drifting pebbles, treated as large dust grains in the chemical network, i.e., with a reduced surface area per H. The inclusion of this advection leads to varying dust-to-gas ratios and varying levels of global abundances of elements with respect to H. The main implication for inner disk in situ planet formation is that the gas in this region, inside the water ice line, is expected to be enriched in oxygen, i.e., a super-Solar abundance, thus driving the C/O ratio down to values as low as ~ 0.1. If this gas is accreted by forming planets, then these abundance patterns may be inherited by the planetary atmospheres and be a

key signature of models of in situ planet formation (e.g., Chatterjee & Tan, 2014).

Simulations of colliding and non-colliding GMCs, similar to those presented in Paper II, but with a range of initial magnetic field strengths from 10 to 50 μG have been carried out. The main work on studying the influence of magnetic field strength on the core mass function (Hsu et al., in prep.) and on the structural and clustering properties of the cores (García-Alvarado, Hsu et al., in prep.) is underway. The simulations have also been used as a training set for machine learning methods, especially a new diffusion model, to predict mass-weighted density from column density maps (Xu et al., submitted).

CHAPTER 6

Concluding Remarks and Future Work

In this thesis, we have performed a series of chemodynamical simulations of star-forming molecular clouds. We have investigated two set-ups: isolated massive prestellar cores, which may be the progenitors of massive stars; giant molecular clouds, including colliding and non-colliding cases, which form overdense clumps that may be the progenitors of star clusters. The aim has been to understand whether these formation mechanisms exhibit particular physical and chemical signatures which can be diagnosed in observations. In addition, we have explored how their physical and chemical properties vary with environmental conditions, such as magnetic field strength, dynamical conditions (i.e., colliding or non-colliding regions), and cosmic ray ionization rate. With the focus of our interest on astrochemical modeling and given the computational cost of coupling large reaction networks to MHD simulations, we have also examined and developed methods for the implementation of such calculations and investigated ways of enhancing the performance of the computations.

In Paper I, we investigated whether the observed high levels of deuterium fractionation in candidate massive pre-stellar cores (PSCs) can be reproduced in an isolated, fast-collapsing, massive cloud. After an extensive parameter

study, we found that a very high CO depletion factor ($f_D \sim 1000$) and relatively high cosmic ray ionization rate ($\zeta \sim 10^{-16}\,\mathrm{s}^{-1}$) are required. However, such a fast collapsing core would tend to exhibit quite disturbed kinematics in its N_2D^+ line emission, which may not be consistent with the few examples of known massive PSCs. Furthermore, our method, which did not include gas-grain processes and treated depletion as a parameter, may yield solutions that are not fully self-consistent. For example, the required high cosmic ray ionization rate may be incompatible with a high CO depletion factor, if cosmic-ray-induced desorption processes are efficient at liberating CO from dust grain ice mantles. Thus further work is needed to investigate deuteration in massive PSCs with a more explicit implementation of gas-grain interactions. An exploration of different physical systems is also warranted. In particular, models that involve relatively slow collapse, mediated by stronger magnetic fields and including non-ideal MHD processes, such as ambipolar diffusion, need to be investigated. In such slower collapsing models there is more time to achieve a given level of deuteration and so lower cosmic ray ionization rates and lower CO depletion factors may be allowed.

In Paper II and related simulations, we investigated whether the cloud-cloud collision mechanism is an effective way to form protoclusters, clumps and populations of PSCs. In particular, we studied the CMFs from high-resolution simulations and compared them with the results from protoclusters, IRDCs, and massive clumps. Clumps formed from cloud collisions are more efficient at producing dense cores and tend to form a relatively top-heavy CMF compared to the Salpeter distribution. We also demonstrated how the results are influenced by the method of observation, especially via synthetic ALMA-type observations. However, both colliding and non-colliding cases can generate CMFs that are consistent with observed populations, so it is difficult to distinguish between these scenarios by this metric. There are many remaining challenges in this topic. The role of different magnetic field strengths has begun to be investigated with an otherwise identical simulation set-up. The effects on the spatial distribution, e.g., clustering, mass segregation, and properties of filaments are also under investigation. It should be noted that our simulations do not yet include star formation or feedback and so are relevant mostly for pre-stellar core populations. In addition, when comparing to observations, one should be aware that most of the CMF studies in distant regions with ALMA, which detect sources via their dust continuum emission, are sen-

sitive to internally heated protostellar cores. Thus, for a fair comparison, new observational samples that exclude protostellar sources are needed. Inclusion of a chemical network that models deuteration in these types of simulations would also be helpful to give additional diagnostics for the PSCs.

In Paper III, we have studied the chemical evolution in colliding and non-colliding GMCs with a gas-grain network, also exploring a range of cosmic ray ionization rates. The simulations generate many important results for the abundances of a variety of species relevant to observations of GMCs on a global scale, but also in their dense clumps and cores. One main observational comparison we have made is with the abundances of CO, HCO^+ and N_2H^+ in the dense clumps of an IRDC. For this we also post-processed our simulations to predict the strength of rotational line emission from these species. In general, the clumps formed in the simulation of colliding GMCs are moderately warmer, $\sim 20\,\mathrm{K}$, than those observed in the IRDC, which are $\lesssim 15\,\mathrm{K}$. This difference could be important in causing the CO depletion factor in our simulated clumps to be lower than the observed regions by factors of a few. Clumps in non-colliding GMCs are somewhat cooler and thus, in this respect, may be a better match to the observed system. However, we note that there is a likely effect of resolution: when running higher resolution simulations, e.g., from Paper II, that does not include active chemistry, we find greater amounts of dense, cooler gas in a given region. Thus, there is a need for higher-resolution chemodynamical simulations, perhaps involving a re-zooming technique that extracts regions of interest from the large-scale domain. The other abundance results of our simulated dense clumps indicate a preference for relatively low cosmic ray ionization rates to explain the HCO^+ abundance, but not too low, else we underpredict N_2H^+. The resolution of this may involve a combination of having higher resolution, denser, cooler clumps, i.e., with better resolved dense substructures and/or indicate that updates are needed in the chemical model, especially for how cosmic rays promote desorption from ice mantles. Another result from our study is a comparison of our modeling and abundance results with those based on single grid chemical modeling of the dense clumps. This comparison reveals important limitations of the static single grid post-processing method that is commonly employed: it is subject to inaccuracies given that it does not track the dynamical history, including advection of material into the region.

Several avenues for improvement of the modeling methods and new investi-

gations are already mentioned above. In addition, there are processes associated with shocks and dust grain sputtering, which are desirable to implement, especially for study of GMC collisions and protostellar outflows. These models are needed to explain the abundances of chemical species, such as SiO, which are expected to be liberated from grains in shocked regions. Another desired improvement is to link the calculated chemical abundances with adaptive heating and cooling functions, i.e., that respond to the chemical evolution. The simulations we have presented here are either approximately isothermal (Paper I) or use pre-computed PDR-model heating and cooling functions, which are not fully consistent with the chemical evolution. Future work is needed to improve self-consistency in this regard.

Finally, for the work presented in this thesis, we have developed the `Naunet` software package. It supports multiple reaction formats, multiple depletion, desorption, surface reaction models and has the flexibility to be customized. It also supports multiple ODE solvers. `Naunet` is planned for public release in the near future.

References

Ahnert, Karsten, Denis Demidov, & Mario Mulansky (2014). "Solving ordinary differential equations on GPUs". In: *Numerical Computations with GPUs*, pp. 125–157. ISBN: 9783319065489.

Alves, J., M. Lombardi, & C. J. Lada (Jan. 2007). "The mass function of dense molecular cores and the origin of the IMF". In: *Astronomy & Astrophysics* 462.1, pp. L17–L21.

Balos, Cody J et al. (2021). "Enabling GPU accelerated computing in the SUNDIALS time integration library". In: *Parallel Computing* 108, p. 102836.

Bastian, Nate, Kevin R. Covey, & Michael R. Meyer (2010). "A universal stellar initial mass function? a critical look at variations". In: *Annual Review of Astronomy and Astrophysics* 48, pp. 339–389. ISSN: 00664146.

Bate, Matthew R., Ian A. Bonnell, & Volker Bromm (Mar. 2003). "The formation of a star cluster: predicting the properties of stars and brown dwarfs". In: *Monthly Notices of the Royal Astronomical Society* 339.3, pp. 577–599.

Bergin, Edwin A. & Mario Tafalla (2007). "Cold Dark Clouds: The Initial Conditions for Star Formation". In: *Annual Review of Astronomy and Astrophysics* 45.1, pp. 339–396. ISSN: 0066-4146.

Bertoldi, Frank & Christopher F. McKee (Aug. 1992). "Pressure-confined clumps in magnetized molecular clouds". In: *The Astrophysical Journal* 395, p. 140. ISSN: 0004-637X.

Beuther, H. et al. (Feb. 2006). "The Formation of Massive Stars". In: *Proceedings of the International Astronomical Union* 6.S270, pp. 57–64.

Bisbas, Thomas G. et al. (2017). "GMC Collisions as Triggers of Star Formation. V. Observational Signatures". In: *The Astrophysical Journal* 850.1, p. 23. ISSN: 1538-4357.

Bonnell, I A et al. (2001). "Competitive accretion in embedded stellar clusters". In: *Monthly Notices of the Royal Astronomical Society* 323.4, pp. 785–794. ISSN: 00358711.

Bovino, S. et al. (2019). "The 3D Structure of CO Depletion in High-mass Prestellar Regions". In: *The Astrophysical Journal* 887.2, p. 224. ISSN: 1538-4357.

Branca, L & A Pallottini (Dec. 2022). "Neural networks: solving the chemistry of the interstellar medium". In: *Monthly Notices of the Royal Astronomical Society* 518.4, pp. 5718–5733. ISSN: 0035-8711.

Brummel-Smith, Corey et al. (Oct. 2019). "ENZO: An Adaptive Mesh Refinement Code for Astrophysics (Version 2.6)". In: *Journal of Open Source Software* 4.42, p. 1636. ISSN: 2475-9066.

Brünken, Sandra et al. (Dec. 2014). "H_2D^+ observations give an age of at least one million years for a cloud core forming Sun-like stars". In: *Nature* 516.7530, pp. 219–221.

Bryan, Greg L. et al. (Apr. 2014). "ENZO: An Adaptive Mesh Refinement Code for Astrophysics". In: *The Astrophysical Journal Supplement Series* 211.2, 19, p. 19.

Butler, Michael J. & Jonathan C. Tan (July 2012). "Mid-infrared Extinction Mapping of Infrared Dark Clouds. II. The Structure of Massive Starless Cores and Clumps". In: *The Astrophysical Journal* 754.1, 5, p. 5.

Caselli, P. et al. (2002). "Molecular Ions in L1544. I. Kinematics". In: *The Astrophysical Journal* 565.1, pp. 331–343. ISSN: 0004-637X.

Ceccarelli, Cecilia et al. (Mar. 2014). "Deuterium Fractionation: the Ariadne's Thread from the Pre-collapse Phase to Meteorites and Comets today". In.

Cevallos Soto, Arturo et al. (Dec. 2022). "Inside-out planet formation - VII. Astrochemical models of protoplanetary discs and implications for planetary compositions". In: *Monthly Notices of the Royal Astronomical Society* 517.2, pp. 2285–2308.

Chabrier, Gilles (July 2003). "Galactic Stellar and Substellar Initial Mass Function". In: *Publications of the Astronomical Society of the Pacific* 115.809, pp. 763–795.

Chatterjee, Sourav & Jonathan C. Tan (Jan. 2014). "Inside-out Planet Formation". In: *The Astrophysical Journal* 780.1, 53, p. 53.

Chen, Ricky T. Q. et al. (June 2018). "Neural Ordinary Differential Equations". In: *arXiv e-prints*, arXiv:1806.07366, arXiv:1806.07366.

Cheng, Yu et al. (2018). "The Core Mass Function in the Massive Protocluster G286.21+0.17 Revealed by ALMA". In: *The Astrophysical Journal* 853.2, p. 160. ISSN: 1538-4357.

Cheng, Yu et al. (Aug. 2021). "Star Formation in a Strongly Magnetized Cloud". In: *The Astrophysical Journal* 916.2, 78, p. 78.

Chevance, Mélanie et al. (2020). "The Molecular Cloud Lifecycle". In: *Space Science Reviews* 216.4. ISSN: 15729672.

Collings, Mark P. et al. (2004). "A laboratory survey of the thermal desorption of astrophysically relevant molecules". In: *Monthly Notices of the Royal Astronomical Society* 354.4, pp. 1133–1140. ISSN: 00358711.

Cosentino, G. et al. (2018). "Widespread SiO and CH3OH emission in filamentary infrared dark clouds". In: *Monthly Notices of the Royal Astronomical Society* 474.3, pp. 3760–3781. ISSN: 13652966.

Crapsi, A. et al. (Jan. 2005). "Probing the Evolutionary Status of Starless Cores through N_2H^+ and N_2D^+ Observations". In: *The Astrophysical Journal* 619.1, pp. 379–406.

Cuppen, H. M. et al. (2017). "Grain Surface Models and Data for Astrochemistry". In: *Space Science Reviews* 212.1-2, pp. 1–58. ISSN: 15729672.

Curtis, Nicholas J., Kyle E. Niemeyer, & Chih-Jen Sung (July 2016). "An investigation of GPU-based stiff chemical kinetics integration methods". In: *Combustion and Flame* 179, pp. 312–324. ISSN: 15562921.

Dalgarno, A. (Sept. 2008). "A serendipitous journey." In: *Annual Review of Astronomy and Astrophysics* 46, pp. 1–20.

Dame, T. M., Dap Hartmann, & P. Thaddeus (Feb. 2001). "The Milky Way in Molecular Clouds: A New Complete CO Survey". In: *The Astrophysical Journal* 547.2, pp. 792–813.

De Mijolla, D. et al. (2019). "Incorporating astrochemistry into molecular line modelling via emulation". In: *Astronomy & Astrophysics* 630. ISSN: 14320746.

Dewangan, L K (May 2022). "New evidences in IRDC G333.73 + 0.37: colliding filamentary clouds, hub-filament system, and embedded cores". In:

Monthly Notices of the Royal Astronomical Society 513.2, pp. 2942–2957. ISSN: 0035-8711.

Dobbs, C. L., J. E. Pringle, & A. Duarte-Cabral (2015). "The frequency and nature of 'cloud-cloud collisions' in galaxies". In: *Monthly Notices of the Royal Astronomical Society* 446.4, pp. 3608–3620. ISSN: 13652966.

Dobbs, C. L. et al. (2014). "Formation of Molecular Clouds and Global Conditions for Star Formation". In: *Protostars and Planets VI* 3.

Dobbs, Clare L., Ian A. Bonnell, & Paul C. Clark (2005). "Centrally condensed turbulent cores: Massive stars or fragmentation?" In: *Monthly Notices of the Royal Astronomical Society* 360.1, pp. 2–8. ISSN: 00358711.

Draine, B. T. (Apr. 1978). "Photoelectric heating of interstellar gas." In: *The Astrophysical Journal Supplement Series* 36, pp. 595–619.

Draine, Bruce T. (2011). *Physics of the Interstellar and Intergalactic Medium.*

Egan, M. P. et al. (1998). "A Population of Cold Cores in the Galactic Plane". In: *The Astrophysical Journal* 494.2, pp. L199–L202. ISSN: 0004637X.

Entekhabi, N. et al. (2022). "Astrochemical modelling of infrared dark clouds". In: *Astronomy & Astrophysics* 662. ISSN: 14320746.

Flower, D. R., G. Pineau Des Forêts, & C. M. Walmsley (Apr. 2006). "The importance of the ortho:para H_2 ratio for the deuteration of molecules during pre-protostellar collapse". In: *Astronomy & Astrophysics* 449.2, pp. 621–629.

Fukui, Yasuo et al. (June 2018). "A New Look at the Molecular Gas in M42 and M43: Possible Evidence for Cloud-Cloud Collision that Triggered Formation of the OB Stars in the Orion Nebula Cluster". In: *The Astrophysical Journal* 859.2, 166, p. 166.

Fukui, Yasuo et al. (2021). "Cloud–cloud collisions and triggered star formation". In: *Publications of the Astronomical Society of Japan* 73, S1–S34. ISSN: 2053051X.

Galván-Madrid, Roberto et al. (Dec. 2010). "From the Convergence of Filaments to Disk-outflow Accretion: Massive Star Formation in W33A". In: *The Astrophysical Journal* 725.1, pp. 17–28.

Gardner, David J et al. (2022). "Enabling new flexibility in the SUNDIALS suite of nonlinear and differential/algebraic equation solvers". In: *ACM Transactions on Mathematical Software (TOMS).*

Garrod, R. T., V. Wakelam, & E. Herbst (June 2007). "Non-thermal desorption from interstellar dust grains via exothermic surface reactions". In: *Astronomy & Astrophysics* 467.3, pp. 1103–1115.

Glover, S. C.O. et al. (2010). "Modelling CO formation in the turbulent interstellar medium". In: *Monthly Notices of the Royal Astronomical Society* 404.1, pp. 2–29. ISSN: 00358711.

Goncalves, Vinicius, Kathia Maria, & Alberico Borges Ferreira da Silv (Jan. 2013). "Applications of Artificial Neural Networks in Chemical Problems". In: *Artificial Neural Networks - Architectures and Applications*. InTech.

Goodson, Matthew D et al. (Sept. 2016). "Structure, Dynamics and Deuterium Fractionation of Massive Pre-Stellar Cores". In: *The Astrophysical Journal* 833.2, p. 274. ISSN: 1538-4357.

Grassi, T et al. (Sept. 2012). "Complexity reduction of astrochemical networks". In: *Monthly Notices of the Royal Astronomical Society* 425.2, pp. 1332–1340. ISSN: 00358711.

Grassi, T. et al. (2014). "KROME-a package to embed chemistry in astrophysical simulations". In: *Monthly Notices of the Royal Astronomical Society* 439.3, pp. 2386–2419. ISSN: 13652966.

Grassi, T. et al. (Apr. 2017). "A detailed framework to incorporate dust in hydrodynamical simulations". In: *Monthly Notices of the Royal Astronomical Society* 466.2, pp. 1259–1274. ISSN: 0035-8711.

Habing, H. J. (Jan. 1968). "The interstellar radiation density between 912 A and 2400 A". In: *Bulletin of the Astronomical Institutes of the Netherlands* 19, p. 421.

Hasegawa, Tatsuhiko I. & Eric Herbst (Mar. 1993). "New gas-grain chemical models of quiscent dense interstellar clouds :the effects of H2 tunnelling reactions and cosmic ray induced desorption." In: *Monthly Notices of the Royal Astronomical Society* 261, pp. 83–102.

Hasegawa, Tatsuhiko I. & Eric Herbst (1993). "Three-phase chemical models of dense interstellar clouds: gas, dust particle mantles and dust particle surfaces". In: *Monthly Notices of the Royal Astronomical Society* 263, p. 589.

Hasegawa, Tatsuhiko I., Eric Herbst, & Chun M. Leukng (1992). "Models of gas-grain chemistry in dense interstellar clouds with complex organic molecules". In: *The Astrophysical Journal Supplement Series* 82, p. 167. ISSN: 0067-0049.

Hennebelle, P. et al. (Apr. 2011). "Collapse, outflows and fragmentation of massive, turbulent and magnetized prestellar barotropic cores". In: *Astronomy & Astrophysics* 528, A72, A72.

Hennebelle, Patrick & Gilles Chabrier (Sept. 2008). "Analytical Theory for the Initial Mass Function: CO Clumps and Prestellar Cores". In: *The Astrophysical Journal* 684.1, pp. 395–410.

Herbst, Eric & Ewine F. Van Dishoeck (2009). "Complex organic interstellar molecules". In: *Annual Review of Astronomy and Astrophysics* 47, pp. 427–480. ISSN: 00664146.

Hincelin, U. et al. (2013). "Survival of interstellar molecules to prestellar dense core collapse and early phases of disk formation". In: *The Astrophysical Journal* 775.1. ISSN: 15384357.

Hincelin, U. et al. (2016). "Chemical and Physical Characterization of Collapsing Low-Mass Prestellar Dense Cores". In: *The Astrophysical Journal* 822.1, p. 12. ISSN: 0004-637X.

Hindmarsh, Alan C et al. (2005). "SUNDIALS: Suite of nonlinear and differential/algebraic equation solvers". In: *ACM Transactions on Mathematical Software (TOMS)* 31.3, pp. 363–396.

Holdship, J. et al. (2017). "UCLCHEM: A Gas-grain Chemical Code for Clouds, Cores, and C-Shocks". In: *The Astronomical Journal* 154.1, p. 38. ISSN: 0004-6256.

Honvault, P. et al. (July 2011). "Ortho-Para H_2 Conversion by Proton Exchange at Low Temperature: An Accurate Quantum Mechanical Study". In: *Physical Review Letters* 107.2, 023201, p. 023201.

Hugo, Edouard, Oskar Asvany, & Stephan Schlemmer (Apr. 2009). "$H_3{}^+$+H_2 isotopic system at low temperatures: Microcanonical model and experimental study". In: *Journal of Chemical Physics* 130.16, pp. 164302–164302.

Jiménez-Serra, I. et al. (2010). "Parsec-scale SiO emission in an infrared dark cloud". In: *Monthly Notices of the Royal Astronomical Society* 406.1, pp. 187–196. ISSN: 13652966.

Kahn, F. D. (Dec. 1974). "Cocoons around early-type stars." In: *Astronomy & Astrophysics* 37, pp. 149–162.

Kennicutt, Robert C & Neal J. Evans (2012). *Star formation in the milky way and nearby galaxies.*

Kong, Shuo et al. (May 2015). "The Deuterium Fractionation Timescale in Dense Cloud Cores: A Parameter Space Exploration". In: *The Astrophysical Journal* 804.2, 98, p. 98.

Kong, Shuo et al. (2016). "the Deuterium Fraction in Massive Starless Cores and Dynamical Implications". In: *The Astrophysical Journal* 821.2, p. 94. ISSN: 1538-4357.

Kong, Shuo et al. (Nov. 2018). "Zooming in to Massive Star Birth". In: *The Astrophysical Journal* 867.2, p. 94. ISSN: 1538-4357.

Körtgen, Bastian et al. (Aug. 2017). "Deuterium fractionation and H_2D^+ evolution in turbulent and magnetized cloud cores". In: *Monthly Notices of the Royal Astronomical Society* 469.3, pp. 2602–2625.

Kroupa, Pavel, Sverre Aarseth, & Jarrod Hurley (Mar. 2001). "The formation of a bound star cluster: from the Orion nebula cluster to the Pleiades". In: *Monthly Notices of the Royal Astronomical Society* 321.4, pp. 699–712.

Krumholz, Mark R. (Nov. 2015). "Notes on Star Formation". In: *arXiv e-prints*, arXiv:1511.03457, arXiv:1511.03457.

Krumholz, Mark R. & Christopher F. McKee (Feb. 2008). "A minimum column density of $1 g cm^{-2}$ for massive star formation". In: *Nature* 451.7182, pp. 1082–1084.

Lam, S H (Mar. 1993). "Using CSP to Understand Complex Chemical Kinetics". In: *Combustion Science and Technology* 89.5-6, pp. 375–404. ISSN: 0010-2202.

Leger, A., M. Jura, & A. Omont (Mar. 1985). "Desorption from interstellar grains". In: *Astronomy & Astrophysics* 144.1, pp. 147–160.

Li, Qi et al. (2018). "The interstellar medium and star formation of galactic disks. I. Interstellar medium and giant molecular cloud properties with diffuse far-ultraviolet and cosmic-ray backgrounds". In: *Publications of the Astronomical Society of Japan* 70, pp. 1–28. ISSN: 2053051X.

Linsky, J. L. (June 2007). "D/H and Nearby Interstellar Cloud Structures". In: *Space Science Reviews* 130.1-4, pp. 367–375.

Liu, Mengyao et al. (2018). "The Core Mass Function across Galactic Environments. II. Infrared Dark Cloud Clumps". In: *The Astrophysical Journal* 862.2, p. 105. ISSN: 0004-637X.

Majumdar, L. et al. (Apr. 2017). "Chemistry of TMC-1 with multiply deuterated species and spin chemistry of H_2, H_2^+, H_3^+ and their isotopologues". In: *Monthly Notices of the Royal Astronomical Society* 466.4, pp. 4470–4479.

Maret, Sébastien & Edwin A. Bergin (July 2015). *Astrochem: Abundances of chemical species in the interstellar medium*. Astrophysics Source Code Library, record ascl:1507.010.

Mathis, J. S., P. G. Mezger, & N. Panagia (Nov. 1983). "Interstellar radiation field and dust temperatures in the diffuse interstellar medium and in giant molecular clouds". In: *Astronomy & Astrophysics* 128, pp. 212–229.

McElroy, D. et al. (Feb. 2013). "The UMIST database for astrochemistry 2012". In: *Astronomy & Astrophysics* 550, A36. ISSN: 0004-6361.

McKee, C. F. & J. P. Ostriker (Nov. 1977). "A theory of the interstellar medium - Three components regulated by supernova explosions in an inhomogeneous substrate". In: *The Astrophysical Journal* 218, p. 148. ISSN: 0004-637X.

McKee, Christopher F. & Eve C. Ostriker (2007). "Theory of Star Formation". In: *Annual Review of Astronomy and Astrophysics* 45.1, pp. 565–687. ISSN: 0066-4146.

McKee, Christopher F. & Jonathan C Tan (Mar. 2003). "The Formation of Massive Stars from Turbulent Cores". In: *The Astrophysical Journal* 585.2, pp. 850–871. ISSN: 0004-637X.

McMullin, J. P. et al. (Oct. 2007). *CASA Architecture and Applications*. Ed. by R. A. Shaw, F. Hill, & D. J. Bell.

Miettinen, O. et al. (2012). "A (sub)millimetre study of dense cores in Orion B9". In: *Astronomy & Astrophysics* 538, pp. 1–20. ISSN: 00046361.

Mouschovias, T. Ch. & Jr. Spitzer, L. (1976). "Note on the collapse of magnetic interstellar clouds". In: *The Astrophysical Journal* 210, pp. 326, 327.

Myers, Andrew T. et al. (Apr. 2013). "The Fragmentation of Magnetized, Massive Star-forming Cores with Radiative Feedback". In: *The Astrophysical Journal* 766.2, 97, p. 97.

Nakamura, Fumitaka et al. (2012). "Evidence for cloud-cloud collision and parsec-scale stellar feedback within the L1641-N region". In: *The Astrophysical Journal* 746.1. ISSN: 15384357.

Nejad, Lida A.M. (2005). "A comparison of stiff ODE solvers for astrochemical kinetics problems". In: *Astrophysics and Space Science* 299.1, pp. 1–29. ISSN: 0004640X.

Nelson, Richard P. & William D. Langer (Oct. 1999). "On the Stability and Evolution of Isolated Bok Globules". In: *The Astrophysical Journal* 524.2, pp. 923–946. ISSN: 0004-637X.

Niemeyer, Kyle E. & Chih-Jen Sung (Jan. 2014). "Accelerating moderately stiff chemical kinetics in reactive-flow simulations using GPUs". In: *Journal of Computational Physics* 256, pp. 854–871.

Offner, S. S. R. et al. (2014). "The Origin and Universality of the Stellar Initial Mass Function". In: *Protostars and Planets VI*.

Ohashi, Satoshi et al. (Dec. 2016). "Dense Core Properties in the Infrared Dark Cloud G14.225-0.506 Revealed by ALMA". In: *The Astrophysical Journal* 833.2, 209, p. 209.

O'Neill, Theo J. et al. (2021). "The Core Mass Function across Galactic Environments. III. Massive Protoclusters". In: *The Astrophysical Journal* 916.1, p. 45. ISSN: 0004-637X.

Padoan, Paolo & Åke Nordlund (Sept. 2002). "The Stellar Initial Mass Function from Turbulent Fragmentation". In: *The Astrophysical Journal* 576.2, pp. 870–879.

Pagani, L. et al. (May 2007). "Depletion and low gas temperature in the L183 (=L134N) prestellar core: the $N2H^+$-$N2D^+$ tool". In: *Astronomy & Astrophysics* 467.1, pp. 179–186.

Pagani, L. et al. (Feb. 2009). "Chemical modeling of L183 (L134N): an estimate of the ortho/para H_2 ratio". In: *Astronomy & Astrophysics* 494.2, pp. 623–636.

Prasad, S. S. & S. P. Tarafdar (Apr. 1983). "UV radiation field inside dense clouds - Its possible existence and chemical implications". In: *The Astrophysical Journal* 267, pp. 603–609.

Rawlings, J. M. C. et al. (1992). "Direct diagnosis of infall in collapsing protostars – I. The theoretical identification of molecular species with broad velocity distributions". In: *Monthly Notices of the Royal Astronomical Society* 255.3, pp. 471–485.

Roberts, J. F. et al. (2007). "Desorption from interstellar ices". In: *Monthly Notices of the Royal Astronomical Society* 382.2, pp. 733–742. ISSN: 00358711.

Roman-Duval, Julia et al. (2010). "Physical properties and galactic distribution of molecular clouds identified in the galactic ring survey". In: *The Astrophysical Journal* 723.1, pp. 492–507. ISSN: 15384357.

Rosolowsky, E. W. et al. (2008). "Structural Analysis of Molecular Clouds: Dendrograms". In: *The Astrophysical Journal* 679.2, pp. 1338–1351. ISSN: 0004-637X.

Ruaud, Maxime, Valentine Wakelam, & Franck Hersant (Apr. 2016). "Gas and grain chemical composition in cold cores as predicted by the Nautilus 3-phase model". In: *Monthly Notices of the Royal Astronomical Society* 459.4, pp. 3756–3767. ISSN: 13652966.

Salpeter, Edwin E. (Jan. 1955). "The Luminosity Function and Stellar Evolution." In: *The Astrophysical Journal* 121, p. 161.

Schive, Hsi Yu et al. (2018). "GAMER-2: A GPU-accelerated adaptive mesh refinement code - Accuracy, performance, and scalability". In: *Monthly Notices of the Royal Astronomical Society* 481.4, pp. 4815–4840. ISSN: 13652966.

Schulz, Norbert S. (2012). *The Formation and Early Evolution of Stars*.

Scoville, N. Z., D. B. Sanders, & D. P. Clemens (Nov. 1986). "High-mass star formation due to cloud-cloud collisions". In: *The Astrophysical Journal* 310, p. L77. ISSN: 0004-637X.

Shen, C J et al. (2004). "Cosmic ray induced explosive chemical desorption in dense clouds". In: *Astronomy & Astrophysics* 415.1, pp. 203–215. ISSN: 00046361.

Shu, Frank H., Fred C. Adams, & Susana Lizano (Sept. 1987). "Star Formation in Molecular Clouds: Observation and Theory". In: *Annual Review of Astronomy and Astrophysics* 25.1, pp. 23–81. ISSN: 0066-4146.

Simon, Robert et al. (Dec. 2006). "The Characterization and Galactic Distribution of Infrared Dark Clouds". In: *The Astrophysical Journal* 653.2, pp. 1325–1335. ISSN: 0004-637X.

Sipilä, O., P. Caselli, & J. Harju (2013). "HD depletion in starless cores". In: *Astronomy & Astrophysics* 554, pp. 1–14. ISSN: 00046361.

Sipilä, O., P. Caselli, & J. Harju (Nov. 2019). "Modeling deuterium chemistry in starless cores: full scrambling versus proton hop". In: *Astronomy & Astrophysics* 631, A63, A63.

Sipilä, O. et al. (Jan. 2010). "Modelling line emission of deuterated H_3^+ from prestellar cores". In: *Astronomy & Astrophysics* 509, A98, A98.

Smith, Britton D. et al. (Apr. 2017). "grackle: a chemistry and cooling library for astrophysics". In: *Monthly Notices of the Royal Astronomical Society* 466.2, pp. 2217–2234. ISSN: 0035-8711.

Smith, Rowan J. et al. (Feb. 2020). "The Cloud Factory I: Generating resolved filamentary molecular clouds from galactic-scale forces". In: *Monthly Notices of the Royal Astronomical Society* 492.2, pp. 1594–1613.

Solomon, P. M. et al. (Aug. 1987). "Mass, luminosity, and line width relations of Galactic molecular clouds". In: *The Astrophysical Journal* 319.44, p. 730. ISSN: 0004-637X.

Stone, Christopher P, Andrew T Alferman, & Kyle E Niemeyer (May 2018). "Accelerating finite-rate chemical kinetics with coprocessors: Comparing vectorization methods on GPUs, MICs, and CPUs". In: *Computer Physics Communications* 226, pp. 18–29. ISSN: 00104655.

Tan, Jonathan C. (2000). "Star Formation Rates in Disk Galaxies and Circumnuclear Starbursts from Cloud Collisions". In: *The Astrophysical Journal* 536.1, pp. 173–184. ISSN: 0004-637X.

Tan, Jonathan C. et al. (2013). "The dynamics of massive starless cores with alma". In: *The Astrophysical Journal* 779.2. ISSN: 15384357.

Tan, Jonathan C. et al. (Feb. 2014). "Massive Star Formation". In: *International Astronomical Union Colloquium* 140, pp. 176–184. ISSN: 0252-9211.

Tasker, Elizabeth J. & Jonathan C. Tan (2009). "Star formation in disk galaxies. I. Formation and evolution of giant molecular clouds via gravitational instability and cloud collisions". In: *The Astrophysical Journal* 700.1, pp. 358–375. ISSN: 15384357.

Tielens, A. G. G. M. (2005). *The Physics and Chemistry of the Interstellar Medium*.

Tielens, A. G. G. M. & W. Hagen (Oct. 1982). "Model calculations of the molecular composition of interstellar grain mantles". In: *Astronomy & Astrophysics* 114.2, pp. 245–260.

Tupper, Paul (June 2002). "Adaptive Model Reduction for Chemical Kinetics". In: *BIT* 42, pp. 447–465.

van der Tak, Floris F. S. et al. (Apr. 2020). "The Leiden Atomic and Molecular Database (LAMDA): Current Status, Recent Updates, and Future Plans". In: *Atoms* 8.2, p. 15.

van Dishoeck, Ewine F. & John H. Black (Nov. 1988). "The Photodissociation and Chemistry of Interstellar CO". In: *The Astrophysical Journal* 334, p. 771.

Vastel, C. et al. (Nov. 2012). "Upper limit for the D_2H^+ ortho-to-para ratio in the prestellar core 16293E (CHESS)". In: *Astronomy & Astrophysics* 547, A33, A33.

Vasyunin, A. I. & Eric Herbst (2013). "A unified monte carlo treatment of gas-grain chemistry for large reaction networks. II. A multiphase gas-surface-layered bulk model". In: *The Astrophysical Journal* 762.2. ISSN: 15384357.

Visser, R., E. F. Van Dishoeck, & J. H. Black (2009). "The photodissociation and chemistry of CO isotopologues: Applications to interstellar clouds and circumstellar disks". In: *Astronomy & Astrophysics* 503.2, pp. 323–343. ISSN: 00046361.

Viti, Serena (Mar. 2013). *UCL_CHEM: time and depth dependent gas-grain chemical model*. Astrophysics Source Code Library, record ascl:1303.006.

Wakelam, V. et al. (2012). "A kinetic database for astrochemistry (KIDA)". In: *The Astrophysical Journal Supplement Series* 199.1. ISSN: 00670049.

Wakelam, V. et al. (2015). "The 2014 kida network for interstellar chemistry". In: *The Astrophysical Journal Supplement Series* 217.2, p. 20. ISSN: 00670049.

Wakelam, V. et al. (2017). "Binding energies: New values and impact on the efficiency of chemical desorption". In: *Molecular Astrophysics* 6, pp. 22–35. ISSN: 24056758.

Wakelam, V. et al. (Aug. 2021). "Efficiency of non-thermal desorptions in cold-core conditions. Testing the sputtering of grain mantles induced by cosmic rays". In: *Astronomy and Astrophysics* 652, A63, A63.

Walmsley, C M, D R Flower, & G Pineau Des Forets (2004). "Complete Depletion in prestellar cores". In: *Astronomy & Astrophysics* 418.0718, p. 22. ISSN: 0004-6361.

Walsh, Catherine, T. J. Millar, & Hideko Nomura (2010). "Chemical processes in protoplanetary disks". In: *The Astrophysical Journal* 722.2, pp. 1607–1623. ISSN: 15384357.

– (2013). "Molecular line emission from a protoplanetary disk irradiated externally by a nearby massive star". In: *The Astrophysical Journal Letters* 766.2, pp. 0–7. ISSN: 20418205.

Walsh, Catherine, Hideko Nomura, & Ewine Van Dishoeck (2015). "The molecular composition of the planet-forming regions of protoplanetary disks across the luminosity regime". In: *Astronomy & Astrophysics* 582, pp. 1–28. ISSN: 14320746.

Walsh, Catherine et al. (2012). "Chemical processes in protoplanetary disks. II. on the importance of photochemistry and X-ray ionization". In: *The Astrophysical Journal* 747.2. ISSN: 15384357.

Walsh, Catherine et al. (2014). "Complex organic molecules in protoplanetary disks". In: *Astronomy & Astrophysics* 563, pp. 1–35. ISSN: 00046361.

Willacy, K. (2007). "The Chemistry of Multiply Deuterated Molecules in Protoplanetary Disks. I. The Outer Disk". In: *The Astrophysical Journal* 660.1, pp. 441–460. ISSN: 0004-637X.

Williams, Jonathan P, Leo Blitz, & Christopher F. McKee (Feb. 2000). "The Structure and Evolution of Molecular Clouds: from Clumps to Cores to the IMF". In: pp. 97–120.

Woodall, J. et al. (May 2007). "The UMIST database for astrochemistry 2006". In: *Astronomy & Astrophysics* 466.3, pp. 1197–1204. ISSN: 0004-6361.

Wu, Benjamin et al. (Jan. 2017). "GMC Collisions as Triggers of Star Formation. II. 3D Turbulent, Magnetized Simulations". In: *The Astrophysical Journal* 835.2, p. 137. ISSN: 1538-4357.

Zhou, Yanxiang et al. (2011). "GPU accelerated biochemical network simulation". In: *Bioinformatics* 27.6, pp. 874–876. ISSN: 13674803.